Distribution Agreement

In presenting this thesis as a partial fulfillment of the requirements for a degree from Emory University, I hereby grant to Emory University and its agents the non-exclusive license to archive, make accessible, and display my thesis in whole or in part in all forms of media, now or hereafter now, including display on the World Wide Web. I understand that I may select some access restrictions as part of the online submission of this thesis. I retain all ownership rights to the copyright of the thesis. I also retain the right to use in future works (such as articles or books) all or part of this thesis.

Yono Bulis April 1st, 2024

Synthesis of P1 and Cap-P2 Fragments of Novel SARS-CoV-2 Protease Inhibitors

By

Yono Bulis

Dr. Franck Amblard

Adviser

Chemistry

Dr. Franck Amblard

Adviser

Dr. Matthew Weinschenk

Committee Member

Dr. Richard Himes

Committee Member

2024

Synthesis of P1 and Cap-P2 Fragments of Novel SARS-CoV-2 Protease Inhibitors

By

Yono Bulis

Dr. Franck Amblard

Advisor

Chemistry

An abstract of

a thesis submitted to the Faculty of Emory College of Arts and Sciences

of Emory University in partial fulfillment

of the requirements of the degree of

Bachelor of Science with Honors

Chemistry

2024

Abstract

Synthesis of P1 and Cap-P2 Fragments of Novel SARS-CoV-2 Protease Inhibitors

By Yono Bulis

The Covid-19 pandemic has led to devastating global public health consequences. As a viral, contagious disease, it has caused millions of deaths worldwide and continues to pose a threat to immunocompromised individuals. SARS-CoV-2's use of a main protease to cleave viral polypeptides provides an excellent target for Covid-19 therapeutics due to its low toxicity. Several SARS-CoV-2 peptidomimetic protease inhibitors have been developed to prevent the cleavage of nascent proteins, culminating in approval for Paxlovid (nirmatrelvir) and Xiannuoxin (simnotrelvir). These compounds may not provide ample treatment for potential variants of Covid-19 and likewise exclude many immunocompromised patient groups from their benefits due to lack of potency and a short half-life. The Laboratory of Biochemical Pharmacology is developing and optimizing more potent SARS-CoV-2 inhibitors that offer a more dynamic, enduring solution for Covid-19 patients. We present progress in completing a synthesis of the Cap-P2 fragment and optimizing a synthesis of the P1 fragment, which will eventually be combined and integrated into several SARS-CoV-2 protease inhibitors that are expected to be more potent.

Synthesis of P1 and Cap-P2 Fragments of Novel SARS-CoV-2 Protease Inhibitors

By

Yono Bulis

Dr. Franck Amblard

Adviser

Chemistry

An abstract of

a thesis submitted to the Faculty of Emory College of Arts and Sciences

of Emory University in partial fulfillment

of the requirements of the degree of

Bachelor of Science with Honors

Chemistry

2024

ACKNOWLEDGEMENTS

Shaoman and Peng: Thank you both for your patience as I took the time to learn organic synthesis. Your teaching has made all the difference in my journey as a research chemist. I'm incredibly lucky to have you as my mentors and role models.

Franck: Thank you for welcoming me into the lab and mentoring me for these past two years. It is reassuring to have such a dedicated and steadfast leader as a guide to the world of organic synthesis and medicinal chemistry. I am always thankful for your incredible depth of knowledge, creativity, flexibility, and commitment to my success as a student, researcher, and chemist.

Dr. Schinazi and the Laboratory of Biochemical Pharmacology: Thank you for the opportunity to be a part of such a wonderful lab. I'm incredibly grateful to have been welcomed into such an empathetic and tenured research community. In particular, thank you to Dharmesh, Li, Longhu, Mahesh, Mohammed, Rama, Nicolas, Zahira, Zhe, and Zhang for always being there to teach me new techniques and answer my questions.

Dr. Weinschenk: Chem 203 and 322 would not be the same without you! I'm so thankful to have taken these courses with such an innovative professor. Your commitment to student learning is a key reason why I've decided to pursue organic chemistry in the future. Additionally, I'm grateful to have served as an LA in your classes, where I can firsthand see your process of teaching, which is both an art and a science.

Dr. Himes: I can't imagine what Atwood and Emory Chemistry would look like without your fun personality and your teaching! I'm grateful you're always willing to answer my

spontaneous questions and guide me through difficult coursework. You set a high bar for students, and my research ability has improved all the more for it.

Emory Chemistry Community: To all my professors, teaching assistants, learning assistants, and colleagues within the Department of Chemistry, thank you for your continued support in so many different ways. I'm proud to call myself a chemistry major because of the sterling reputation of this department. Moreover, I'm explicitly thankful for the revamped Unbound curriculum, which has contributed immensely to my learning.

My friends and family: Your support has kept me going through the highs and lows of my thesis. I feel very lucky to be surrounded by a community that is so invested in my success. Thank you and תּוֹדָה רַבָּה.

Table of Contents

Chapter 1: Introduction to the SARS-CoV-2 Protease Inhibitor

1.1. SARS-CoV-2

Since its initial transmission to humans in 2019, Severe Acute Respiratory Syndrome coronavirus 2 (SARS-CoV-2) has led to the devastating global Covid-19 pandemic, resulting in millions of deaths and hospitalizations (Figure 1). Although the pandemic has largely ended as a direct result of the vaccine immunization of the American and global population, Covid-19 still poses a threat. As of March 2024, the CDC estimates that 2.2% of deaths in the United States were due to Covid-19[1]. The now-archived New York Times Outbreak Tracker offers data into the disastrous global consequences of the pandemic (Figure 2)[2].

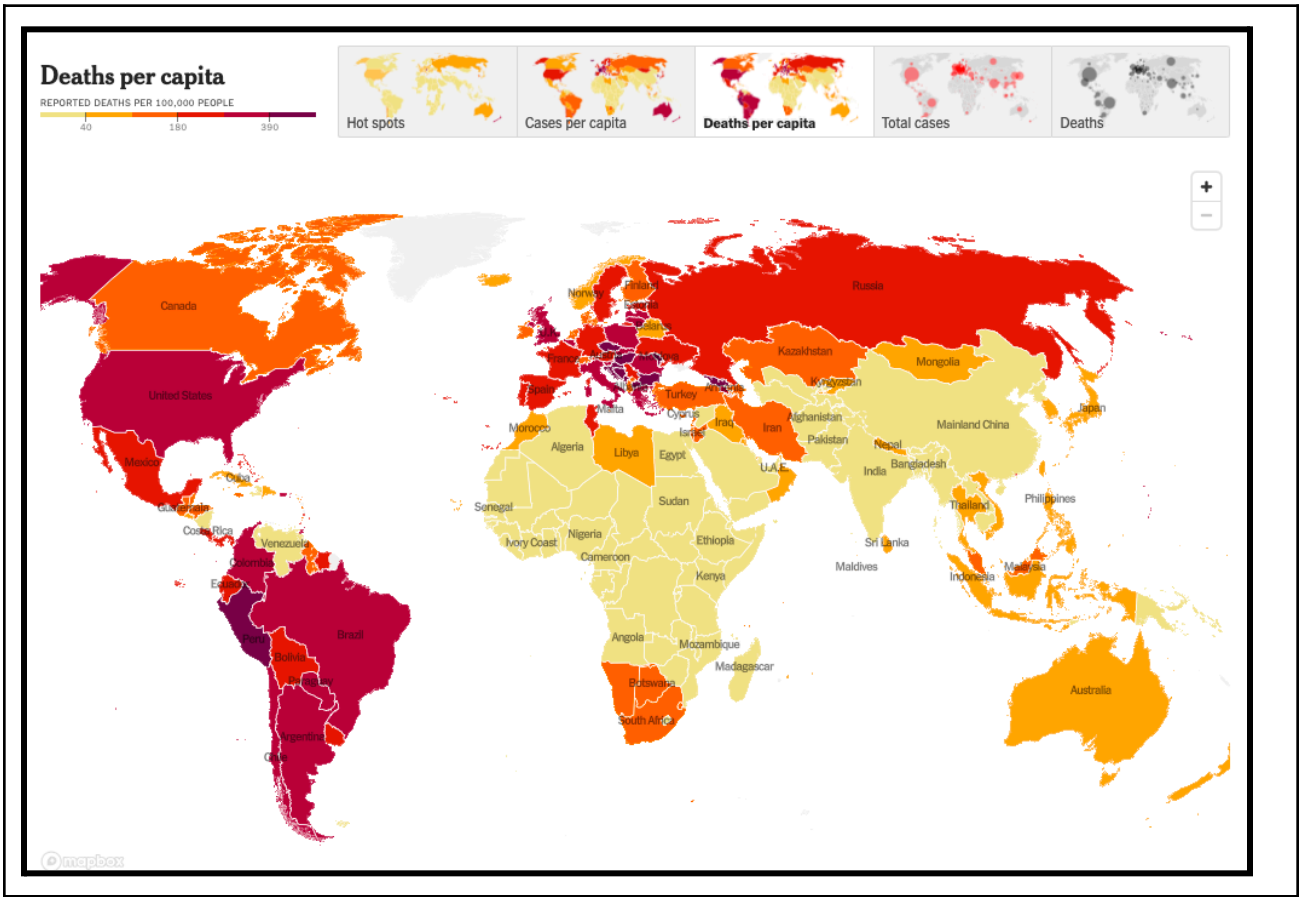

Figure 1: Deaths per capita from the onset of the pandemic until March 2023 demonstrates the pronounced effect of Covid-19 on the United States[1].

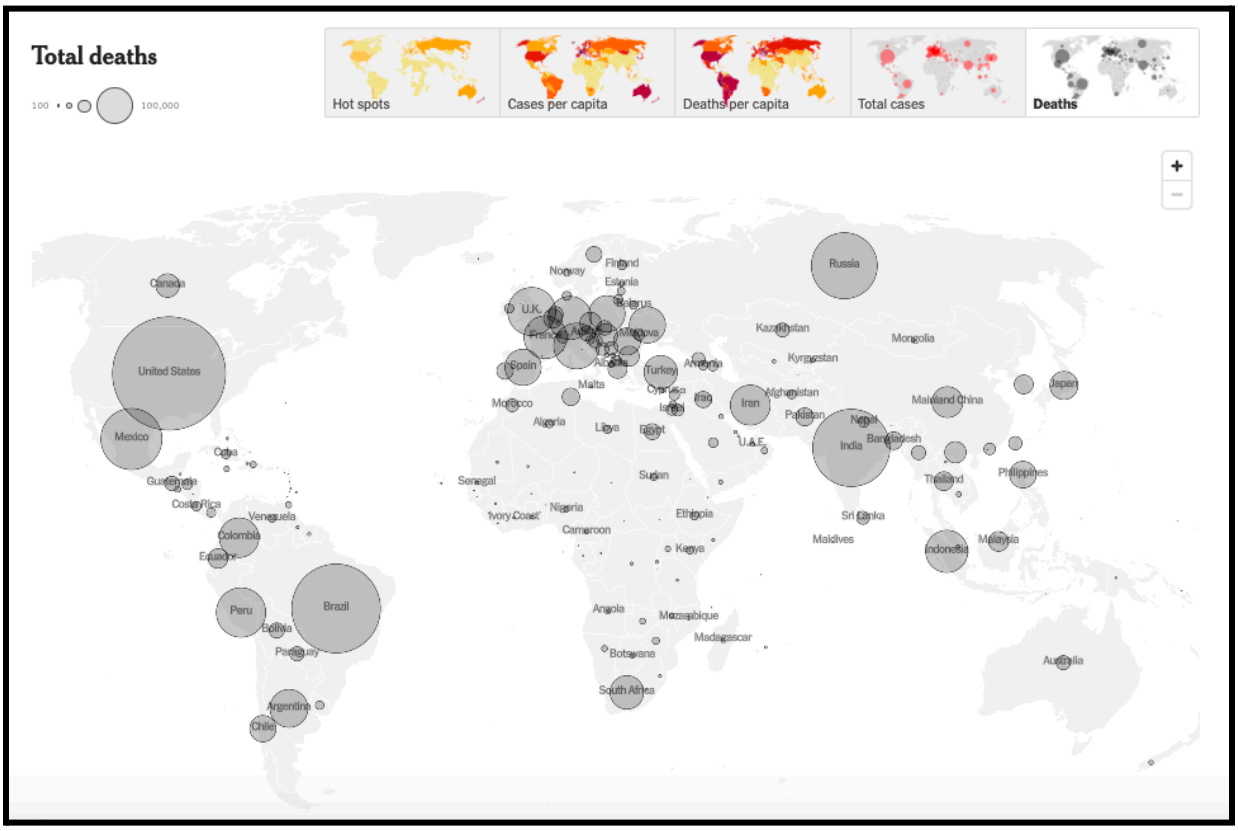

Figure 2: Total deaths from Covid-19, from its onset until March 2023[1].

Covid-19 is a highly contagious virus. On average, an infected person can infect three other individuals, a much higher average than Middle East Respiratory Syndrome (MERS) which infects 1.7-1.9 on average, or South Asian Respiratory Syndrome (SARS) which infects less than 1 on average[3]. Common symptoms of Covid-19 include fever, cough, fatigue, and dyspnea. Although symptoms are typically mild, Covid-19 can lead to respiratory failure, arrhythmia, liver failure, or kidney failure, especially in immunocompromised patients[4].

SARS-CoV-2 is a member of the Coronavirus family of RNA viruses. There have been seven discovered coronaviruses that affect humans, including MERS and SARS. SARS-CoV-2 is a positive-sense, single-stranded RNA virus with a genome size of 29.9 kilobases. A lipid bilayer

membrane and spike proteins form a viral envelope that contains the viral RNA and associated nucleocapsid proteins[5]. The spike proteins facilitate attachment to host cells, whereupon binding triggers the fusion of the viral membrane and the cell membrane. The viral RNA enters the cell membrane, where its ORF1a and ORF1b genes are translated into two viral polypeptides, pp1a (~450 kDa) and pp1ab (~750 kDa). These polypeptides are cleaved by the viral proteases PL^{Pro} and M^{Pro} respectively. RNA-dependent RNA polymerase (RdRP) likewise serves to cleave part of pp1ab[5, 6, 7] (Figure 3). All together, PL^{Pro}, M^{Pro}, and RdRp cleave pp1a and pp1ab into 16 non-structural proteins. Due to their importance in rendering viral functionality, PL^{Pro}, M^{Pro}, and RdRp are key targets for the development of anti-SARS-CoV-2 agents.

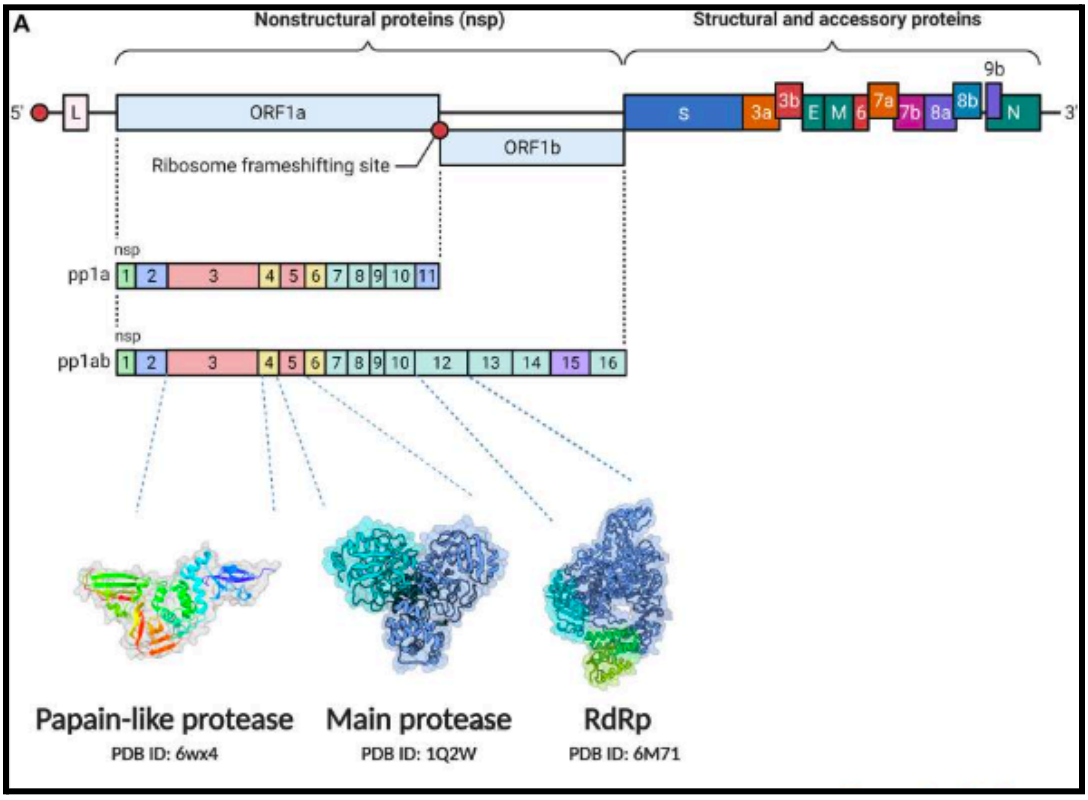

Figure 3: The Papain-like protease (PL^{Pro}) cleaves at pp1a and the main protease (M^{Pro}), and RNA-dependent RNA Polymerase (Rdrp) cleave at pp1ab to form 16 non-structural proteins[7].

The SARS-CoV-2 main protease, Mpro or 3CLPro, is a cysteine protease that enables viral replication by cleaving viral polypeptides. The protease functions with a histidine side group (His^{41}) and a cysteine side group (Cys^{145}) that recognize and cleave the scissile bond between glutamine and serine residues[8] (Figure 4).

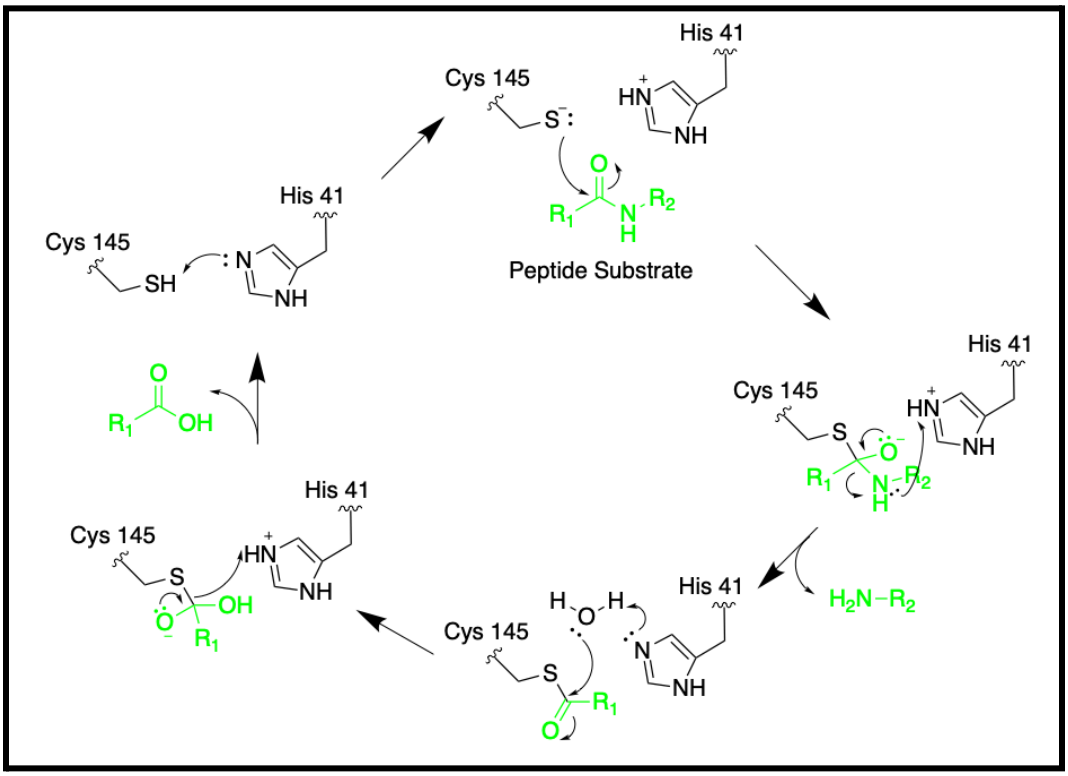

Figure 4: Mechanism of the SARS-CoV-2 Protease[8].

M^{Pro} is a well-characterized drug target and there are currently no human proteases that have been found to have a similar cleavage specificity as the SARS-CoV-2 main protease, which suggests inhibitors would have low toxicity[9]. Inhibitors bind to the active site at Cys^{145}, prevent cleavage of viral polypeptides, and ultimately lead to neutralization of the virus.

1.2. SARS-CoV-2 Protease Inhibitors

The general framework for a peptidomimetic protease inhibitor (Figure 5) is used to inform SAR studies. The peptidomimetic backbone of the inhibitor (P1-P4) mimics the natural substrate and allows for the compound to seat in the active site while the warhead moiety, commonly an electrophilic functional group, undergoes nucleophilic attack by the negatively-charged Cys^{145} group[9]. Following the formation of a covalently bound intermediate, the enzyme is inactivated (Figure 6).

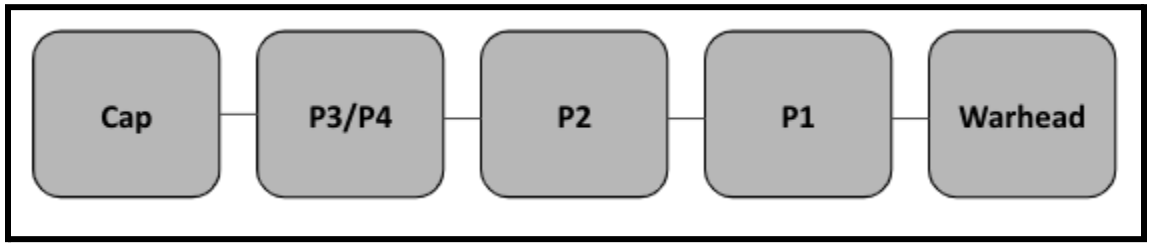

Figure 5: Structural skeleton of a peptidomimetic protease inhibitor[10].

The other fragments of a SARS-CoV-2 protease inhibitor do not interact with the protease. Their role in improving half-life and active site fit are all crucial to the development of a good SARS-CoV-2 compound. The Cap moiety, often a hydrophobic group, allows for permeability across the cellular membrane. P2 mimics the viral polypeptide, often sporting a isopropyl-like moiety that resembles a leucine amino acid, which improves the fit in the binding pocket. P1 likewise improves the steric fit in the M^{Pro} binding pocket. A crystal structure of an α-ketoamide inhibitor complexed to the SARS-CoV-2 M^{Pro} obtained by Zhang et al. illustrates the importance of optimizing each part of the structure in order to achieve optimal potency (Figure 6)[9].

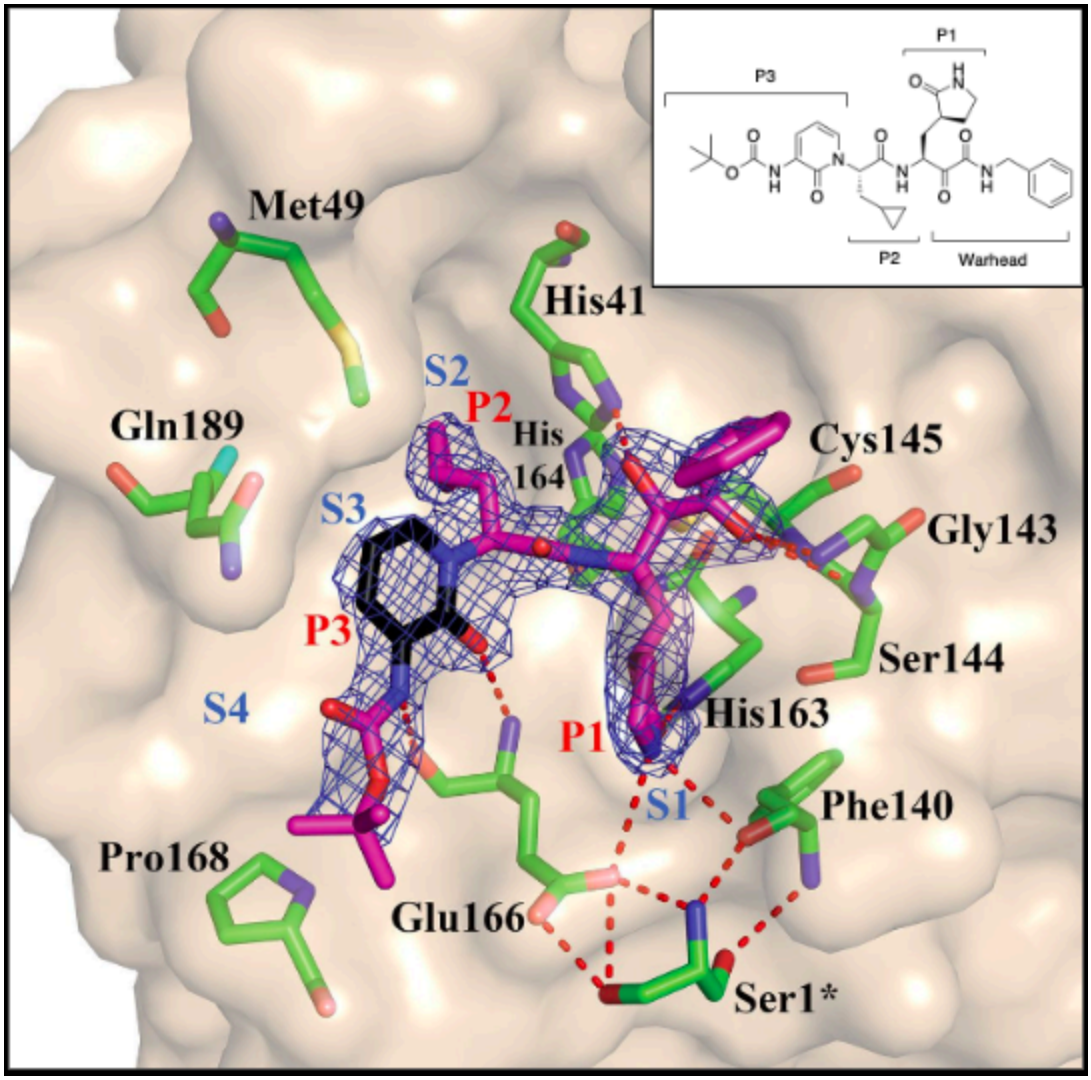

Figure 6: Crystal structure of the pocket interactions between an M^{Pro} inhibitor and the SARS-CoV-2 protease[9].

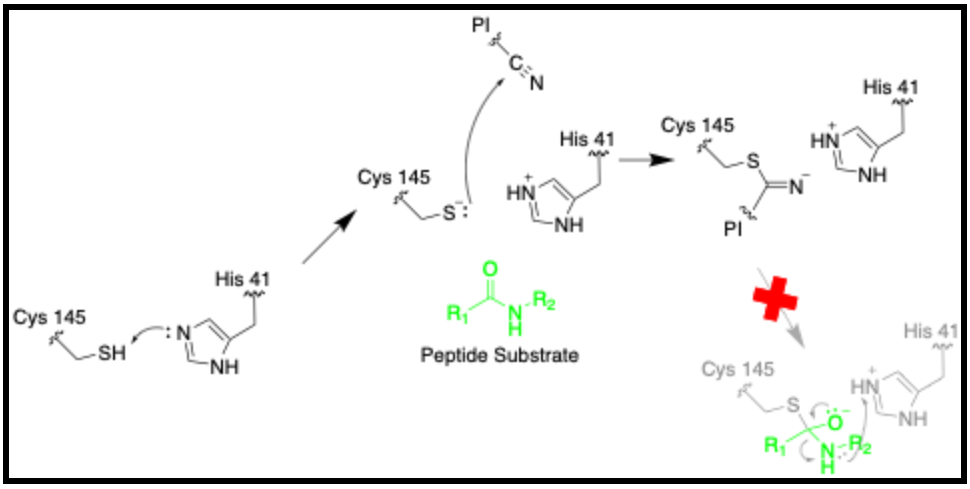

Figure 7: The warhead of peptidomimetic M^{Pro} inhibitors (shown here as a nitrile) covalently binds to Cys^{145} and prevents scission between the nascent viral polypeptide's glutamine and serine residues[11].

Several peptidomimetic compounds with a similar scaffold – often including a piperidinone group at P1, an isobutyl group mimicking Leucine at P2, a napthyl group at P3, and a nitrile group at the warhead – were investigated for potency in both pharmaceutical and academic settings.

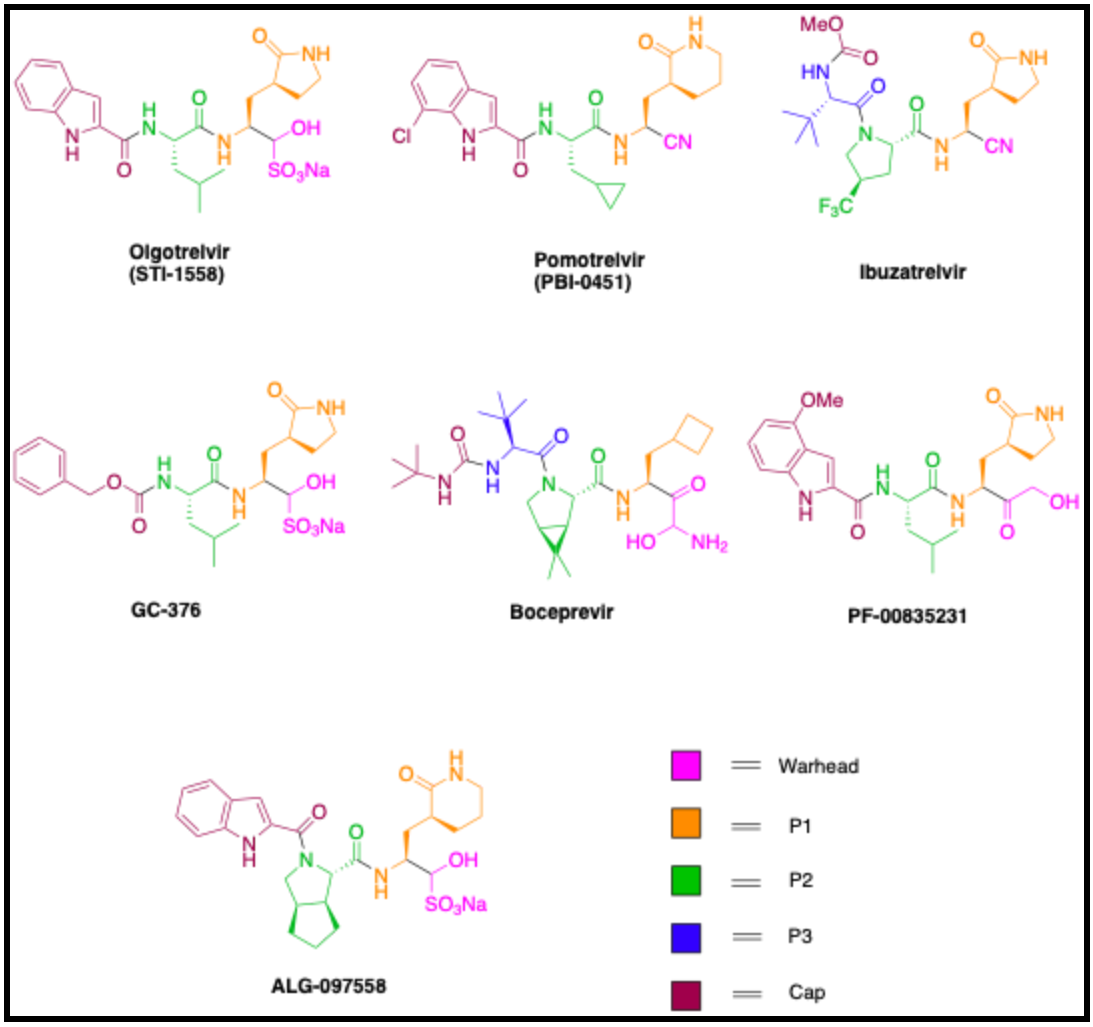

Figure 8: Known M^{Pro} inhibitors[12, 13].

Several M^{Pro} inhibitors with a peptidomimetic backbone have been evaluated at the clinical trial stage (Figure 8)[12, 13]. Simnotrelvir and Nirmatrelvir (Figure 9) are the only ones that have been approved (in China and the United States, respectively), and for the sake of brevity, only their SAR studies will be discussed.

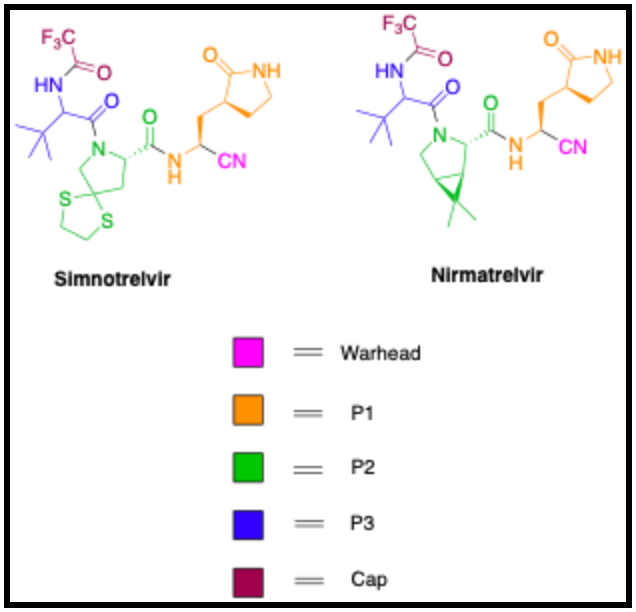

Figure 9: Approved M^{Pro} inhibitors[12, 14, 15,].

The China-based Simcere Pharmaceutical had its M^{Pro} inhibitor, Simnotrelvir, approved in China in January 2023. The company conducted SAR studies starting from Boceprevir, an HCV drug that showed weak inhibition against SARS-CoV-2 M^{Pro}.

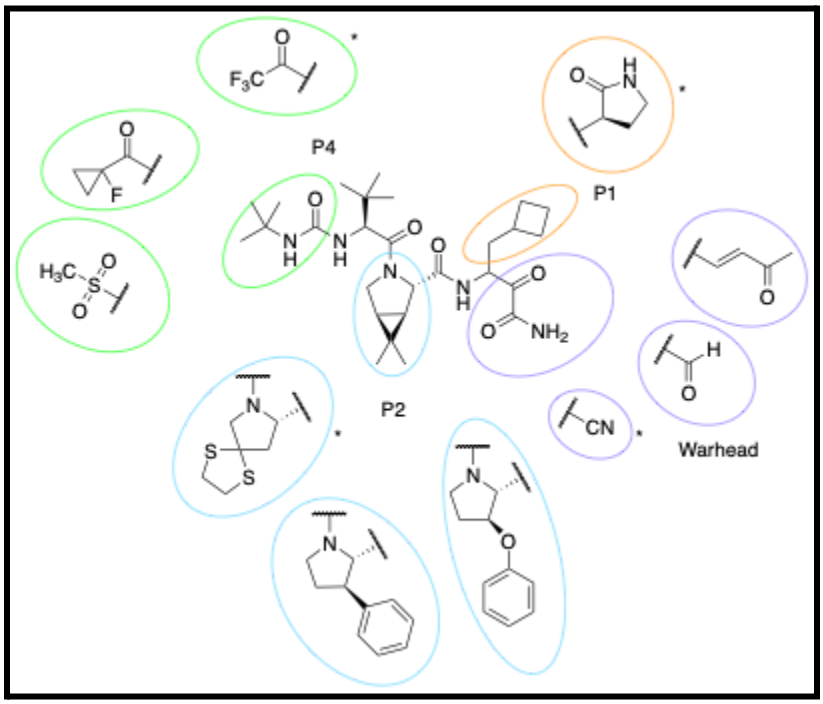

Figure 10: Boceprevir, Simcere's lead compound, with alternative moieties optimized during SAR studies[15].

At the warhead position, Simcere found that the nitrile group provides the best potency in a range of in vitro cell lines and likewise showed low cytotoxicity. At P2, the group found that the dispiro-proline moiety – indicated with an asterisk – had the highest potency out of the other P2 candidate groups. Similarly, at P4, the trifluoroacetyl group – marked with an asterisk – provided the highest potency, as well as negligible toxicity, as compared to the other P4 candidate moieties. Thus, Simcere moved forward with the ideal compound and synthesized Simnotrelvir (Figure 9)[15].

Pfizer's readily made PF-00835231, initially synthesized to treat Severe Acute Respiratory Syndrome (SARS), which serendipitously served to guide their SAR studies in pursuit of a Covid-19 treatment. PF-00835231 showed efficacy against SARS-CoV-2; however, the compound is not orally bioavailable. As a result of its five hydrogen bond donors, it boasts a polar surface area, which traps it in the gut. Thus, Pfizer proceeded with accelerated SAR studies to develop a potent, orally bioavailable compound, focusing on the removal of hydrogen bond donors[16].

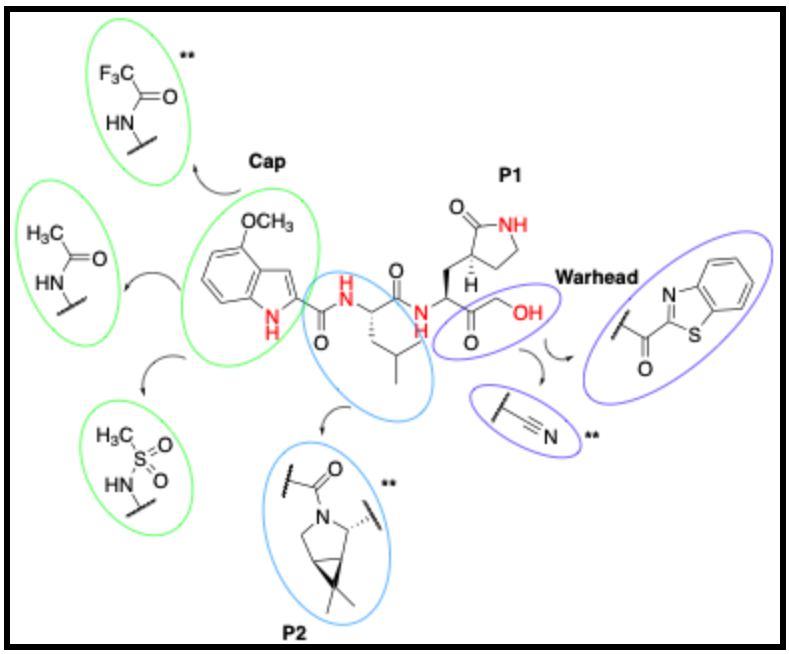

Figure 11: Pfizer's early lead protease inhibitor compound, PF-00835231, with highlighted proton donors and alternative moieties tested in SAR studies[16].

Pfizer developed new compounds that swapped the warhead α-hydroxymethyl ketone with a nitrile and a benzothiazol-2-yl ketone (Figure 11). A functional group with generous electrophilic properties – a π bond, in particular – is critical for the warhead to create a covalent bond with Cys[41] and inhibit the SARS-CoV-2 protease (Figure 6). The nitrile group led to improved solubility, decreased difficulties in epimerization of the adjacent hydrogen, and decreased manufacturing complexity, suggesting it would provide a better fit. Computational studies informed the importance of a leucine-like motif at P2; however, by replacing a true leucine fragment with a cyclic amino acid and a fused cyclopropyl ring with two methyl groups, Pfizer was able to remove a hydrogen bond donor. Although this change led to a modest drop in potency that would prove problematic in later-stage pharmacokinetic studies, the molecule remained active and ultimately the change was kept. At the Cap, trifluoroacetamide stood out compared to other moieties in its ability to permeate the gut barrier in assays, cementing it as the

preferred moiety. At the culmination of Pfizer's SAR, nirmatrelvir was identified as the best protease inhibitor[16].

1.3. Toward the next generation of SARS-CoV-2 Protease inhibitors

Currently, Pfizer's Paxlovid (nirmatrelvir + ritonavir) is the only FDA-approved Covid-19 treatment for individuals who have not been hospitalized. Paxlovid's active compound, nirmatrelvir, suffers from rapid breakdown in the body and has to be administered with ritonavir, a pharmacokinetic boosting agent that decreases the rate of metabolism for nirmatrelvir. Administration of Paxlovid – which is recommended twice a day – consists of two 150 mg nirmatrelvir tablets and one 100 mg ritonavir tablet. Despite the effective solutions to Paxlovid's metabolism problems, many difficulties endure. At-risk patients, such as those with severe kidney or liver diseases, are not recommended Paxlovid due to its high dosage. Simnotrelvir similarly must be taken with ritonavir. Additionally, Paxlovid has contraindications with many drugs across several classes of prevalent conditions and diseases. Finally, some patients endorse a second round of Covid-19 soon after taking Paxlovid-assisted recovery[11, 12, 15]. The obstinate threat of new Covid-19 mutants likewise serves as an incentive for the investigation and pursuit of novel SARS-CoV-2 protease inhibitors, which can provide improved potency against future variants of Covid-19.

1.4. Target Compounds

The Laboratory of Biochemical Pharmacology (LOBP) at Emory has identified several novel peptidomimetic inhibitors including compound 1 (Figure 11). While this compound displays *in vitro* activity similar to that of reference compound nirmatrelvir, its overall stability

remains an issue and would eventually have to be administered in combination with PI booster ritonavir. As part of a drug optimization effort, novel P1 and Cap moieties were designed and synthesized to optimize the overall drug-like properties of lead compound **1** (Figure 12).

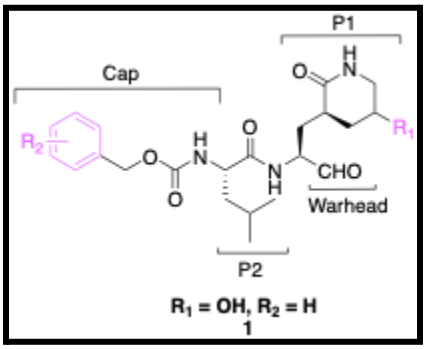

Figure 12: Structure of lead compound 1 and positions selected for optimization.

Chapter 2: Synthesis

2.1. Synthesis of the P1 Subunit

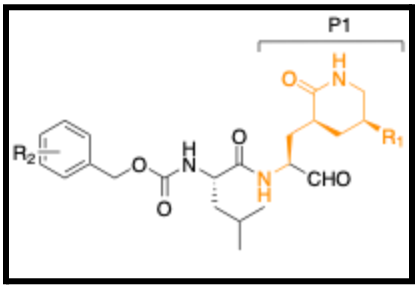

Scheme 1: Target substituted P1 moiety.

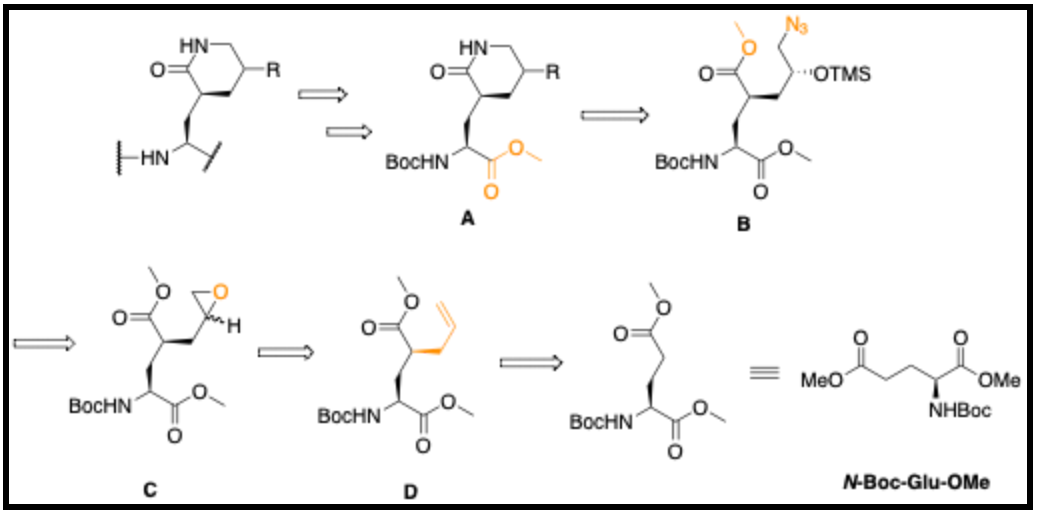

Scheme 2: Envisioned retrosynthesis for the P1 subunit.

Our retrosynthetic approach of the P1 fragment starts from commercially available *N*-Boc-Glu-OMe and uses a key reduction and cyclization sequence to form the 6-membered ring with the desired stereochemistry. The key stereochemistry was introduced with an asymmetric epoxide opening (Scheme 2).

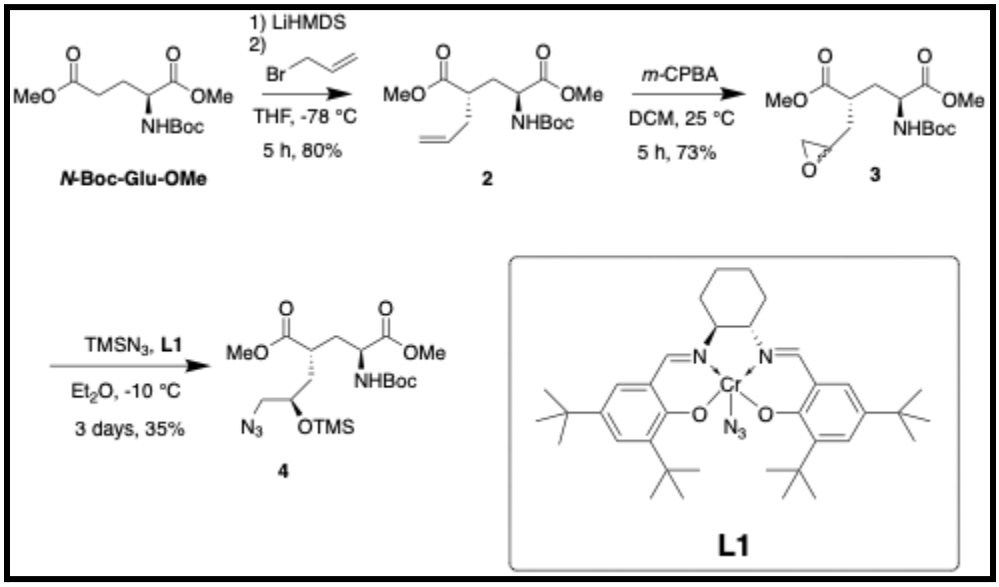

Scheme 3: Synthesis of **4**.

Synthesis of the P1 subunit proceeded via deprotonation with LiHMDS of *N*-Boc-Glu-OMe and then reaction with allyl bromide to afford compound **2** as a single

diastereomer due to the nearby sterically-bulky Boc-protecting group[17]. Compound **2** was reacted with *m*-CPBA to give **3** as a racemic mixture (S:R ratio was found to be 5:1, as determined by ^{1}H NMR). An enantioselective epoxide opening – as outlined by Jacobsen[18, 19]– was identified as the key step, and the necessary ligand **L1** was synthesized (Scheme 4).

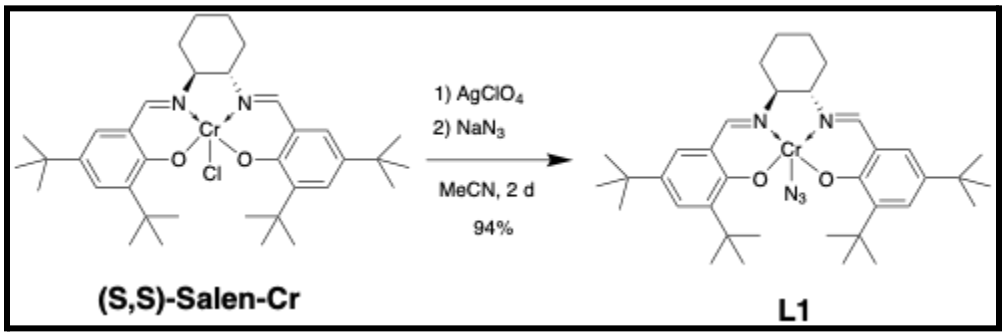

Scheme 4: Synthesis of ligand L1.

The epoxide-opening reaction was undertaken with compound **3** in the presence of **L1** to form **4**, which was detected by LC-MS. Based on the procedure reported by Jacobsen[18, 19] it is expected that L1 only reacts with one stereoisomer, thereby resulting in only one enantiomer of **4** (Scheme 5).

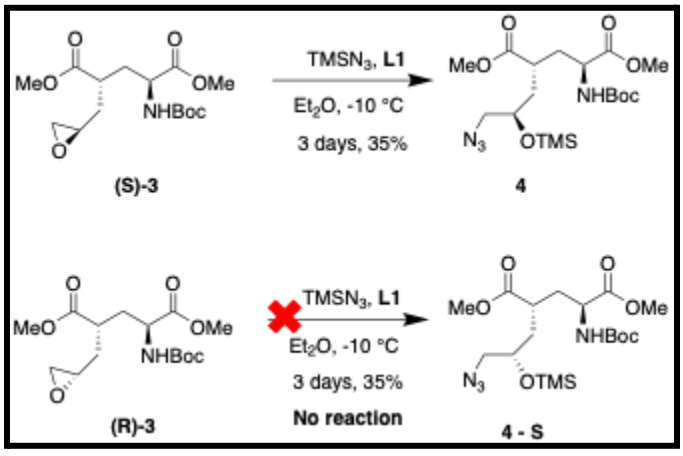

Scheme 5: Reactivity of (S)-3 and (R)-3

Several conditions were evaluated to reduce azido derivative **4** and obtain the desired P1 scaffold **5** (Scheme 6). Hydrogenation at 30 psi in the presence of palladium on charcoal was attempted with modest success: the P1 Subunit scaffold was detected by LC-MS, but several side products were also detected, and much of the starting material remained intact (Scheme 6, Entry 1). An alternative reaction route through a Staudinger azide reduction was evaluated. Unfortunately, none of the conditions used (Scheme 6, Entry 2-5) led to the desired compound, either resulting in a complex mixture of compounds or showing no reaction progress.

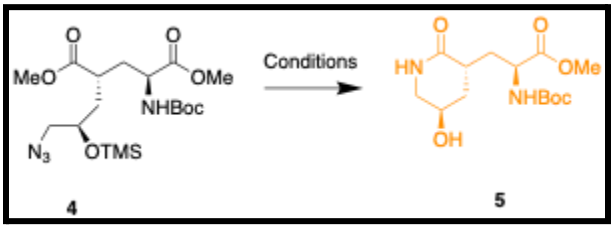

Entry	Conditions	Temperature	Time	Results
1	H_2, Pd/C, MeOH, 30 PSI	25°C	3 days	Detected by LC-MS
2	10% PPh_3, THF/H_2O	25°C	1 day	No reaction
3	10% PPh_3, THF/H_2O	40°C	1 day	No Reaction
4	10% PPh_3, THF/H_2O	60°C	1 day	Decomposition
5	10% PPh_3, THF/H_2O	50°C	1 day	Detected by LC-MS

Scheme 6: Optimization of the reduction/cyclization step.

Based on these negative results, an alternative synthetic route was designed to prepare the P1 subunit (Scheme 7).

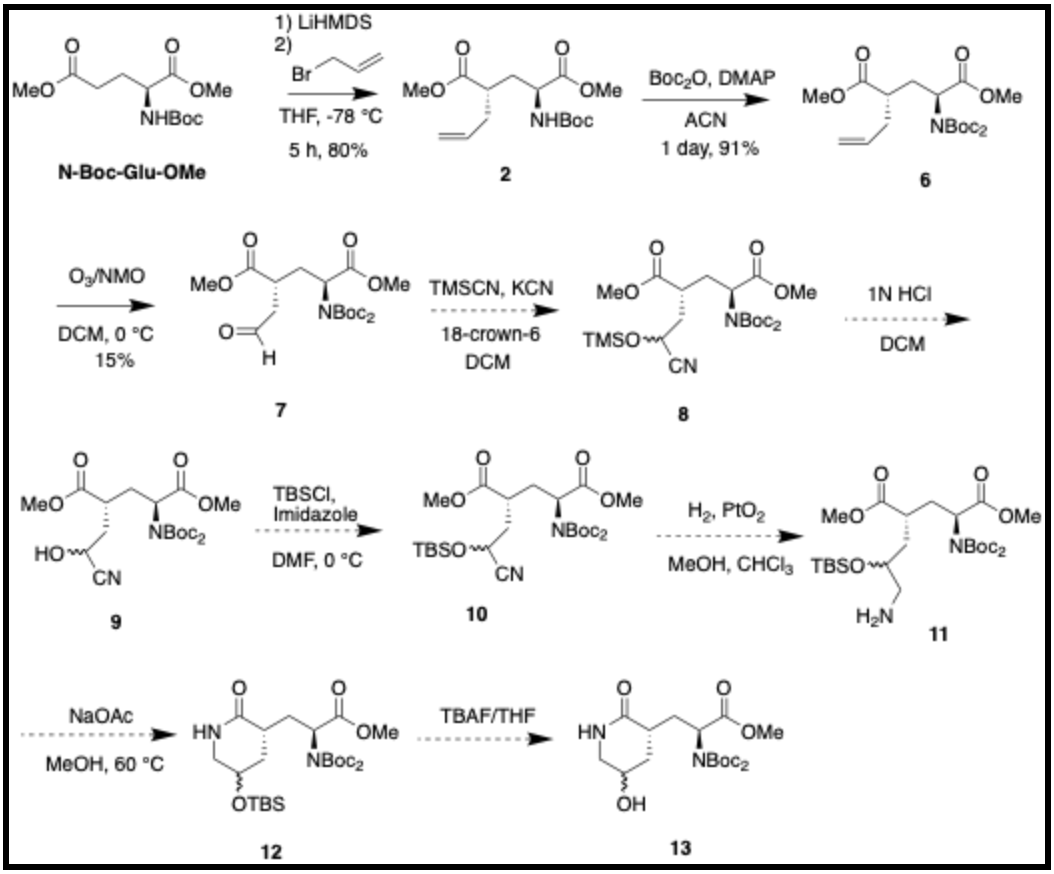

Scheme 7: Alternative synthesis of **13**.

Compound **2** underwent further protection by Boc_2O to yield **6** to prevent the amine proton from interfering with the following oxidation step. **6** underwent ozonolysis in the presence of NMO to yield **7**. Efforts are presently focused on the completion, optimization, and scale-up of this synthetic route.

2.2. Synthesis of the Cap-P2 Subunit

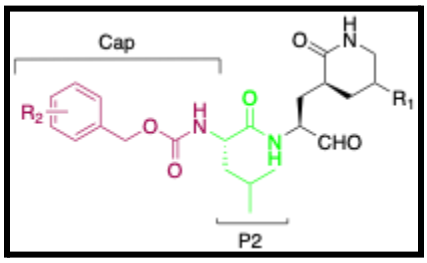

Scheme 8: Target Cap-P2 moiety.

The synthesis of the Cap-P2 Subunit started with the protection of 2-hydroxybenzyl alcohol in the presence of TBSCl and imidazole to give **14**. Alkylation with two different R-Br (substitution confidential) after deprotonation with sodium hydride followed by a straightforward deprotection in the presence of TBAF gave **16** in 25% overall yield.

L-leucine was activated as an isocyanate by reaction with triphosgene in the presence of $NaHCO_3$ and then reacted with **16** in the presence of triethylamine to yield **18** in 98% yield.

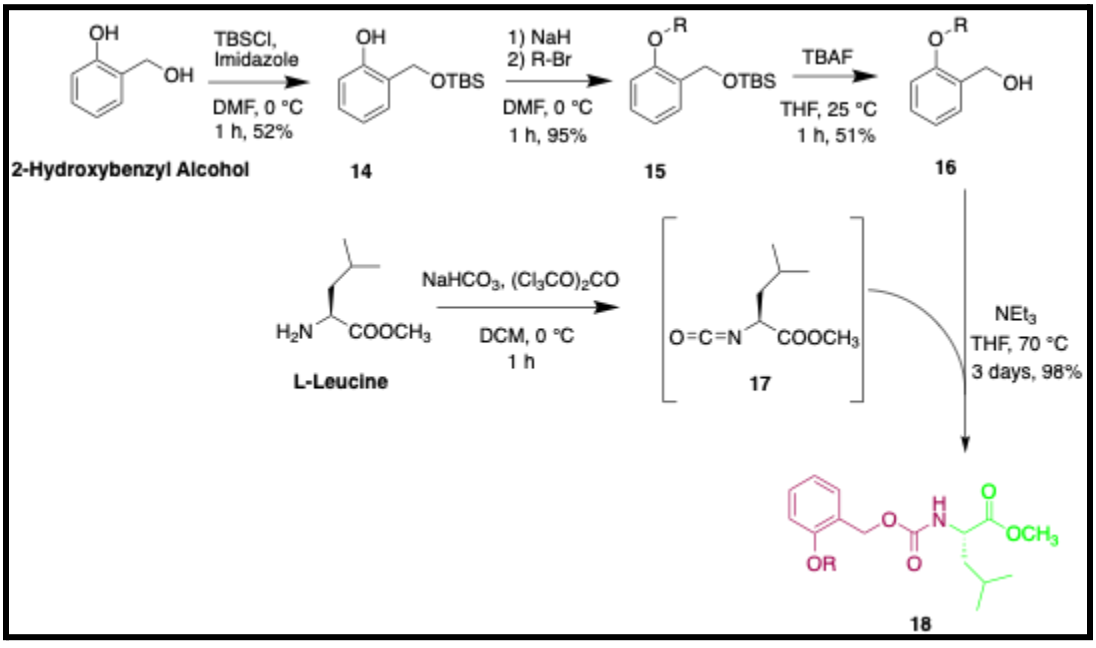

Scheme 9: Synthesis of Cap-P2.

Chapter 3: Conclusions and Future Directions

As part of this project, the following were achieved:

- A robust, convergent synthetic route to prepare several analog Cap-P2 fragments has been developed, and 2 grams of **18** have been isolated and characterized.
- Synthesis of the novel P1 moiety proved to be problematic using our original approach. An alternative synthesis going through a key aldehyde intermediate has been designed and is presently being evaluated to obtain the desired P1 moiety (Scheme 7).

Once the synthesis of P1 is optimized, coupling of the P1 and Cap-P2 moieties followed by further functionalization of the compounds will lead to the desired SARS-CoV-2 protease inhibitors (Scheme 11) which will be evaluated for antiviral activity.

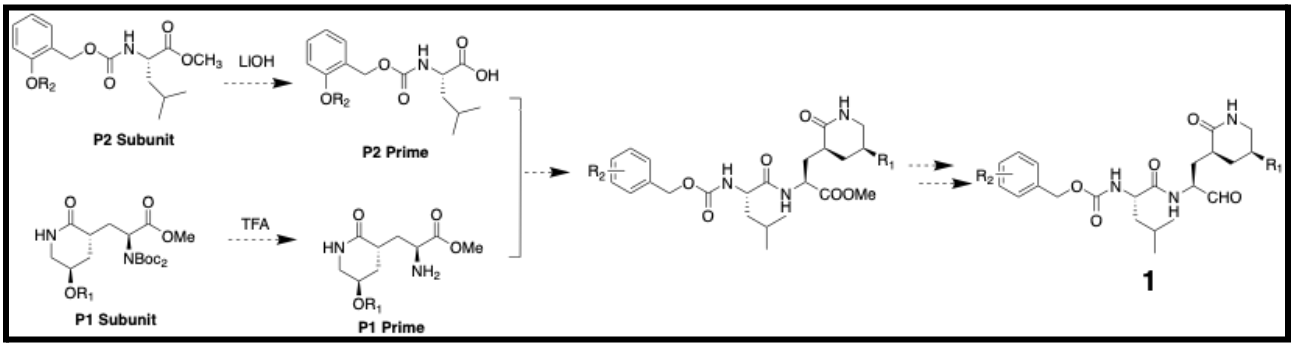

Scheme 10: Synthesis of target SARS-CoV-2 PIs.

Chapter 4: Supporting Information

4.1. General Information

Anhydrous solvents were purchased from Aldrich Chemical Company, Inc. (Milwaukee, Wisconsin, USA). Reagents were purchased from commercial sources. Unless noted otherwise, the materials used in the examples were obtained from readily available commercial suppliers or synthesized by standard methods known to one skilled in the art of organic chemistry synthesis.

1H and 13C spectra were obtained on a Bruker Ascend™ 400 spectrometer (Bruker BioSpin Corporation, Billerica, MA, USA) at room temperature and reported in ppm downfield from internal tetramethylsilane (for 1H NMR). NMR processing was performed with MestReNova version 10.0.2–15465. Deuterium exchange and decoupling experiments were utilized to confirm proton assignments. Signal multiplicities are represented by s (singlet), d (doublet), dd (doublet of doublets), t (triplet), q (quadruplet), br (broad), bs (broad singlet), m (multiplet). All J-values are in Hz and calculated by Mnova or MestReNova programs (V 14.1.1). Mass spectra were determined on a Waters Acquity UPLC using electrospray ionization (Waters Corporation, Milford, MA, USA). Analytic TLC was performed on Analtech GHLF silica gel plates (Analtech, Newark, DE, USA), and preparative TLC on Analtech GF silica gel plates (Analtech, Newark, DE, USA). Column chromatography was performed on Combiflash Rf200 or via reverse-phase high performance liquid chromatography.

4.2. Synthetic procedures

Ligand L1

To a solution of $AgClO_4$ (34.3 mg, 0.17 mmol) in MeCN (4 mL) was added commercially available (S,S)-Salen-Cr (91.4 mg, 0.144 mmol) dissolved in MeCN (4mL) at room temperature dropwise over 5 minutes. The mixture was stirred at room temperature for 16 hours. The mixture was then filtered through a bed of cellite with two 15 mL MeCN washes. The filtrate was concentrated and redissolved in 5 mL of MeCN. NaN_3 (34 mg, 0.52 mmol) was added, and the mixture was stirred at room temperature for 2 days. The mixture was diluted with methyl tert-butyl ether (50 mL), washed three times with H_2O (20 mL). The organic phase was dried with Na_2SO_4, filtered over cellite, and concentrated to give ligand L1 (86.4 mg, 0.135 mmol,

94% yield). No characterization was completed, though a known procedure from Jacobsen et al. was used[18, 19].

Dimethyl (2S,4S)-2-allyl-4-((tert-butoxycarbonyl)amino)pentanedioate (2)

Under an inert atmosphere, commercially available (10.4 g, 0.038 mol) *N*-Boc-Glu-OMe was dissolved in THF (125 mL). LiHMDS (0.038 mol, 38 mL) was added dropwise at -78 ºC, and the reaction was stirred for 1 hour at this temperature. Allyl bromide (0.125 mol) was added over a 30 minute period, and the reaction was stirred for 5 hours at -78 ºC. The mixture was extracted with three 50 mL washes of Ethyl Acetate. The organic layer was concentrated under vacuum, dried with Na_2SO_4, and purified via flash chromatography (Hexane/EA 5:1 to 3:1) to give **2** as a gray oily liquid (8.5 g, 80% yield).

^{1}H NMR (400 MHz, $CDCl_3$) δ 5.65 - 5.76 (m, 3H), 5.10 (s, 1H), 5.01 - 5.06 (m, 2H), 4.33 - 4.38 (dd, 1H), 3.73 (s, 3H), 3.67 (s, 3H), 2.585 (p, J = 8 Hz, 1H), 2.31 - 2.37 (m, 2H), 1.93 - 2.02 (m, 1H), 1.44 (s, 9H).

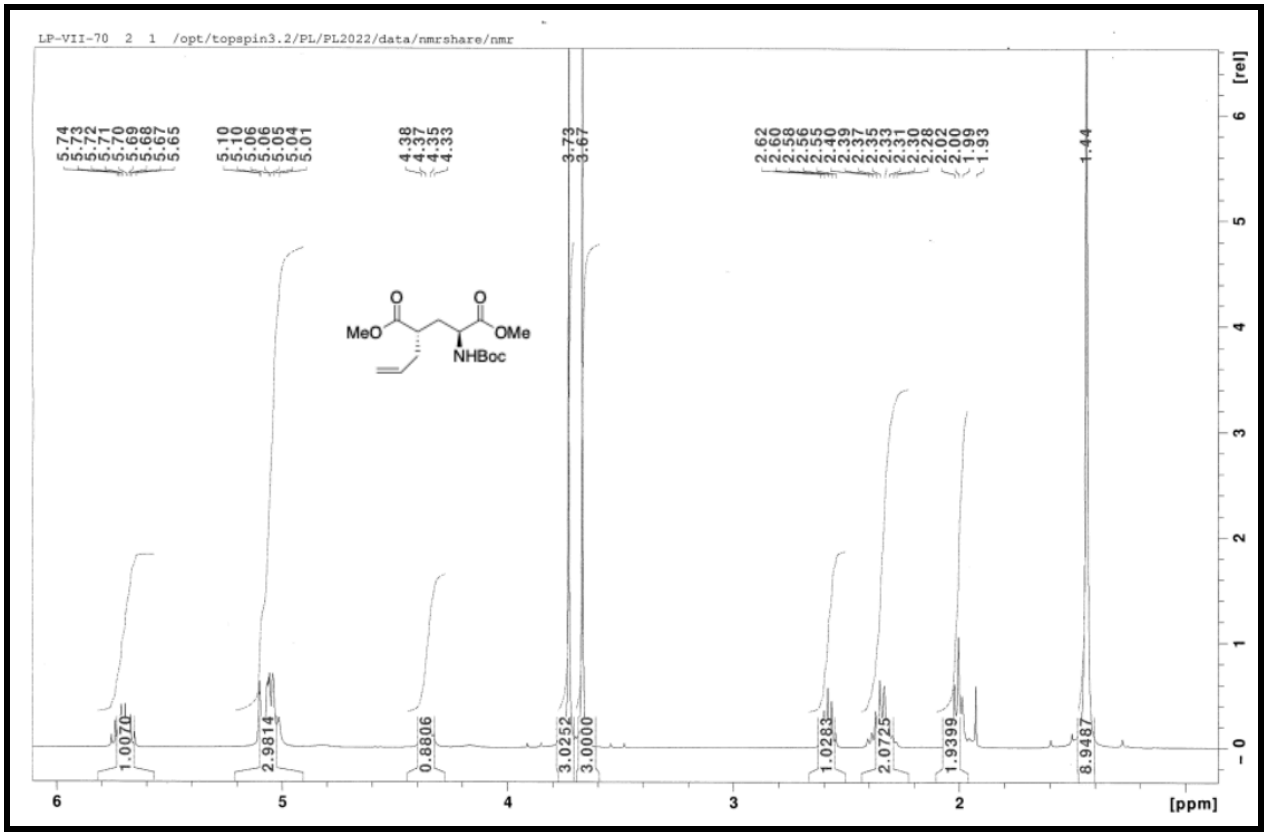

Dimethyl (2S,4R)-2-((tert-butoxycarbonyl)amino)-4-(oxiran-2-ylmethyl)pentanedioate (3)

To a solution of **2** (8.5 g, 0.027 mol) dissolved in DCM (125 mL) *m*CPBA (5.1 g, 0.03 mol) was added under inert atmosphere.The reaction was stirred at room temperature for 5 hours. The resulting mixture was washed three times with ethyl acetate (20mL), dried with Na_2SO_4, concentrated under vacuum, purified via flash chromatography (Hexane/EA 3:1 to 2:1), and isolated to yield **3** (6.6 g, 73% yield).

^{1}H NMR (400 MHz, $CDCl_3$) δ 5.08 (d, *J* = 8 Hz, 1H), 4.35 - 4.42 (m, 1 H), 3.74 (2s, CH_3, 3H), 3.70 (2s, CH_3, 3H), 3.70 (s, 1H), 2.92 - 2.97 (m, 1H), 2.74 - 2.76 (m, 1H), 2.46 - 2.48 (m, 1H), 2.05 - 2.09 (m, 2 H), 1.77 - 1.82 (m, 1H), 1.71 - 1.75 (m, 1H), 1.44 (s, 9H)

^{13}C NMR: δ 175.23, 175.29, 172.66, 155.33, 80.06, 52.42, 52.04, 51.94, 49.98, 46.94, 46.67, 39.80, 39.55, 34.92, 34.85, 34.43, 34.23, 28.25, 27.86.

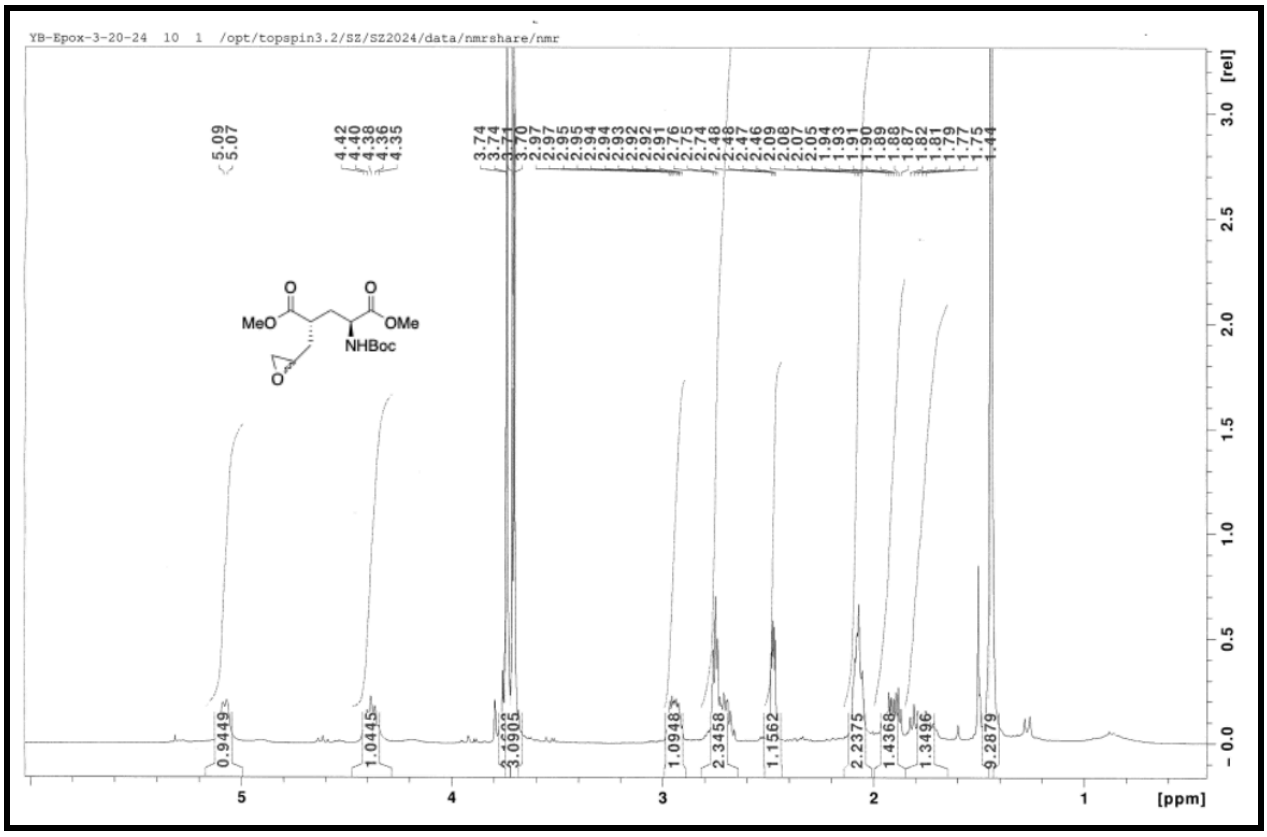
YB-Epox-3-20-24 10 1 /opt/topspin3.2/SZ/SZ2024/data/nmrshare/nmr
MeO
OMe
NHBoc
[ppm]
[rel]

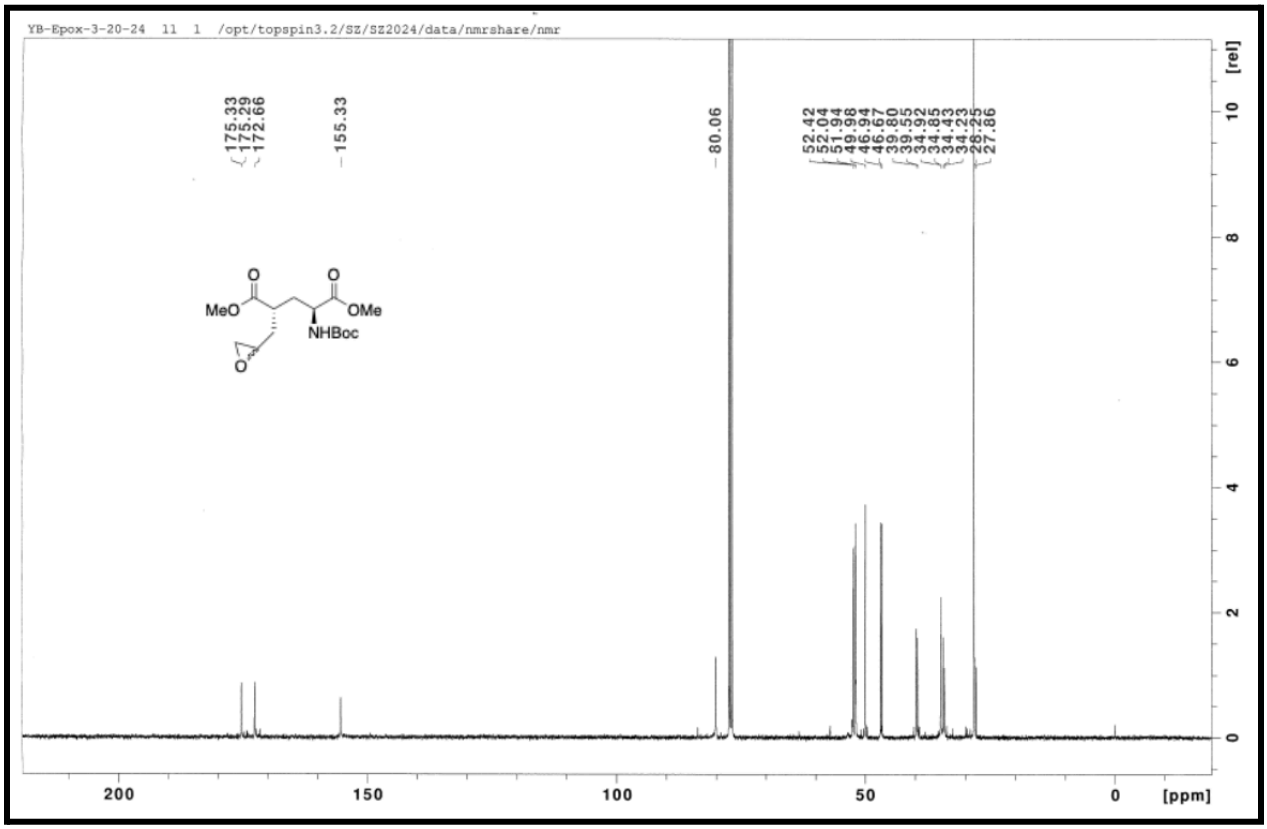
YB-Epox-3-20-24 11 1 /opt/topspin3.2/SZ/SZ2024/data/nmrshare/nmr
MeO
OMe
NHBoc
[ppm]
[rel]

Dimethyl (2R,4S)-2-((R)-3-azido-2-((trimethylsilyl)oxy)propyl)-4-((tert-butoxycarbonyl)amino)pentanedioate (4)

To a solution of **3** (30 mg, 0.1 mmol) in diethyl ether was added L1 (0.1 mg, 0.15 mmol). The reaction was stirred for 5 minutes, and then $TMSN_3$ (0.1 mmol, 0.013 mL) was added. The reaction was stirred at -10 ºC for three days. The mixture was extracted three times with ethyl acetate (2 mL), dried with Na_2SO_4, concentrated under vacuum, and purified by flash chromatography (Hexane/EA 3:1:1 to 2:1) to yield **4** (15 mg, 0.033 mmol, 35% yield) as detected via LC-MS. Due to the small quantity of **4**, further purification and NMR were not undertaken.

MS m/z [M + H]+ calcd for $C_{18}H_{34}N_4O_7Si$: 447.23, found: 447.2.

Dimethyl (2S,4R)-2-(bis(tert-butoxycarbonyl)amino)-4-(2-oxoethyl)pentanedioate (6)

5 (11.58 g, 36.76 mmol) was dissolved in ACN (160 mL). Boc_2O (9.62 g, 44.1 mmol) was added. DMAP (610 mg, 5.0 mmol) was added at 0 ºC. The resulting mixture was stirred at room temperature for one day. The mixture was then concentrated under vacuum and the residue was purified with flash chromatography (Hexane/EA 10:1 to 5:1) to yield **6** (13.9 g, 33.45 mmol, 91% yield).

^1H NMR (400 MHz, $CDCl_3$) δ 5.68 - 5.78 (m, 1H), 4.82 - 5.10 (m, 3H), 3.71 (s, 3H), 3.65 (s, 3H), 2.56 - 2.63 (m, 1H), 2.22 - 2.40 (m, 2H), 1.44 (18H).

^{13}C NMR (400 MHz, $CDCl_3$) δ175.29, 170.98, 151.10, 134.77, 117.29, 83.29, 56.25, 52.21, 51.67, 42.75, 36.60, 31.91, 27.93.

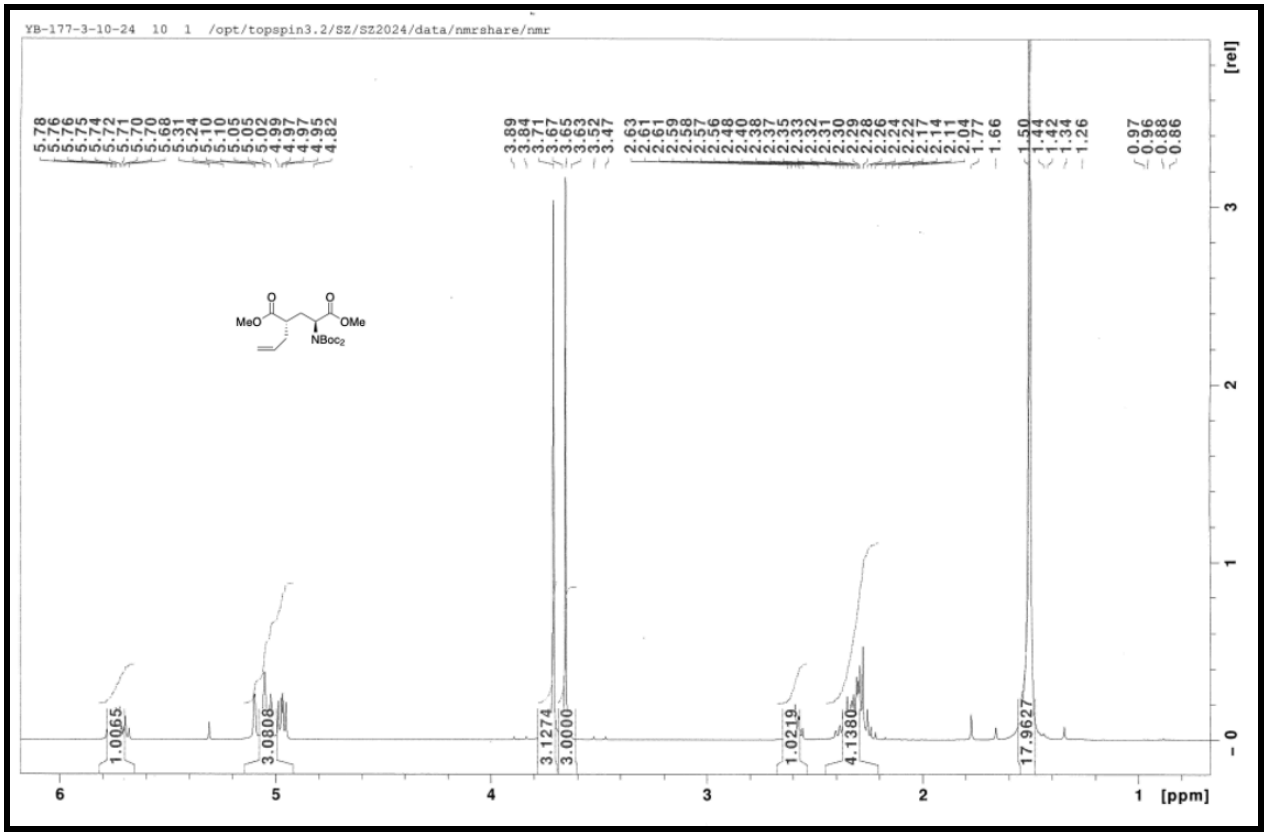
YB-177-3-10-24 10 1 /opt/topspin3.2/SZ/SZ2024/data/nmrshare/nmr
5.78
5.76
5.76
5.75
5.74
5.72
5.71
5.70
5.70
5.68
5.31
5.24
5.10
5.10
5.05
5.02
4.99
4.97
4.97
4.95
4.82
3.89
3.84
3.71
3.67
3.65
3.63
3.52
3.47
2.63
2.61
2.61
2.59
2.58
2.57
2.56
2.48
2.40
2.38
2.37
2.35
2.33
2.32
2.31
2.30
2.29
2.28
2.26
2.24
2.22
2.17
2.14
2.11
2.04
1.77
1.66
1.50
1.44
1.42
1.34
1.26
0.97
0.96
0.88
0.86
MeO
OMe
NBoc2
1.0065
3.0808
3.1274
3.0000
1.0219
4.1380
17.9627
[rel]
[ppm]

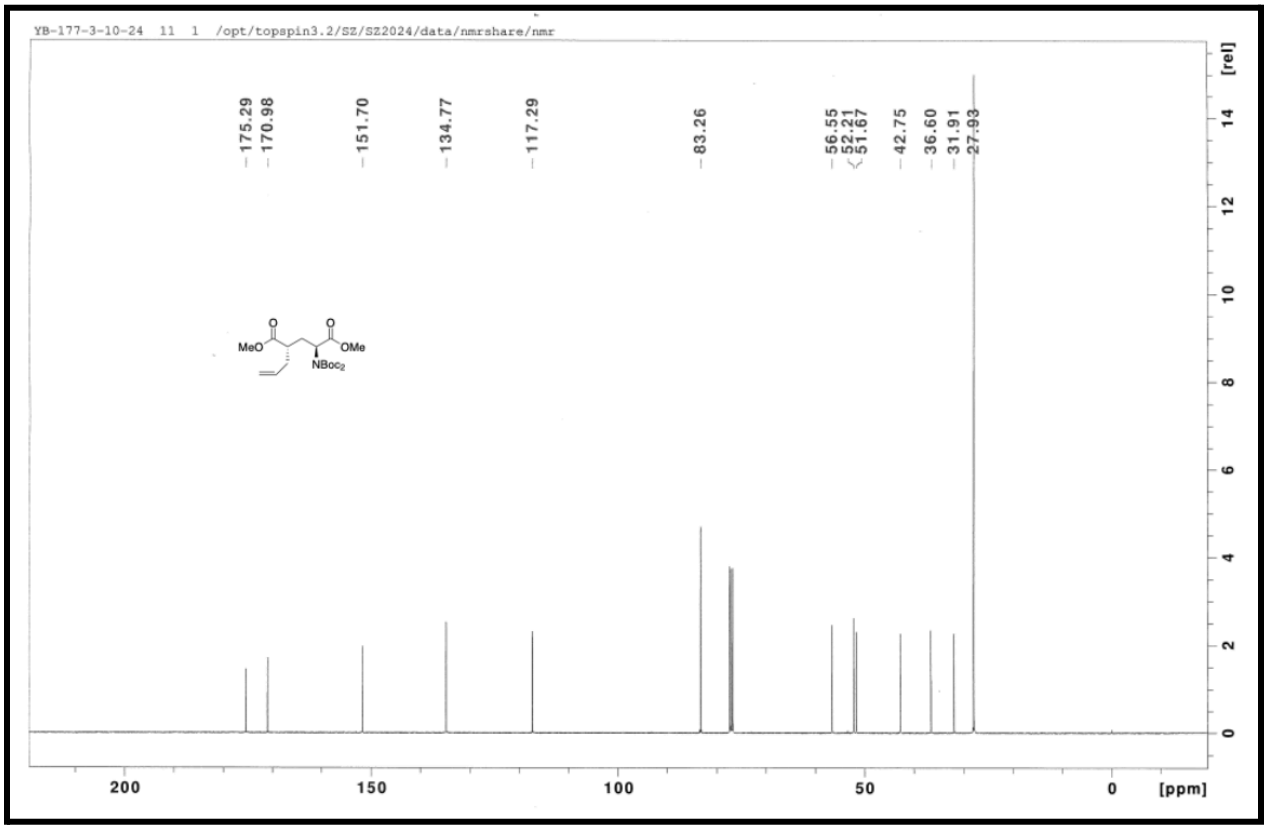
YB-177-3-10-24 11 1 /opt/topspin3.2/SZ/SZ2024/data/nmrshare/nmr
175.29
170.98
151.70
134.77
117.29
83.26
56.55
52.21
51.67
42.75
36.60
31.91
27.93
MeO
OMe
NBoc2
[rel]
[ppm]

Dimethyl (2S,4R)-2-(bis(tert-butoxycarbonyl)amino)-4-(2-oxoethyl)pentanedioate (7)

Compound **6** (3.767 g, 9.38 mmol) was dissolved in DCM (50 mL). NMO (3.23 g, 27.6 mmol) was added. O_3 was introduced through solution continuously at 0 ºC for 1 day, using an A2Z Inc. Ozone Generator. The reaction was monitored using TLC. Following total consumption of the starting material, the resulting mixture was washed three times with H_2O (20 mL), dried with Na_2SO_4, concentrated under vacuum, and purified by flash chromatography (Hexane/EA 5:1:1 to 3:1) to give **7** (530.7 mg, 1.27 mmol, 13.5% yield).

^{1}H NMR (400 MHz, $CDCl_3$) 9.75 (s, 1H), 7.27 (s, 1H), 5.005 (dd, J = 4 Hz, 1H), 4.12 (dd, J = 4 Hz, 1H), 3.72 (s, 3H), 3.69 (s, 3H), 2.86 - 2.98 (m, 2H), 2.72 (dd, J = 4 Hz, 1H), 2.23 - 2.38 (m, 2H), 2.05 (s, 3H), 1.60 (s, H), 1.50 (s, 18H), 1.26 (t, J = 8 Hz, 3 H), 0.00 (s, 1H)

^{13}C NMR (400 MHz, $CDCl_3$) δ199.63, 174.64, 171.14, 170.77, 151.89, 83.59, 60.39, 55.85, 52.38, 52.20, 45.06, 36.37, 31.97, 27.94, 21.05 14.20

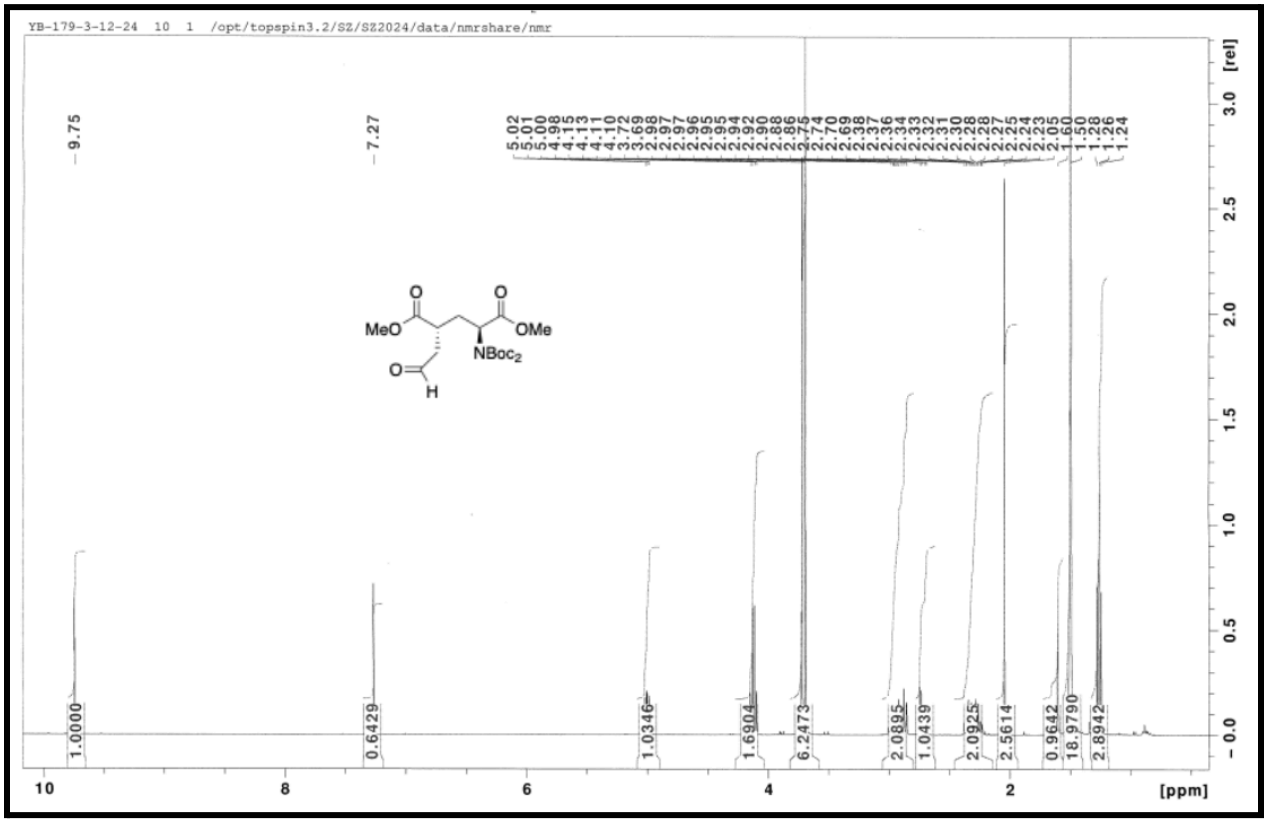

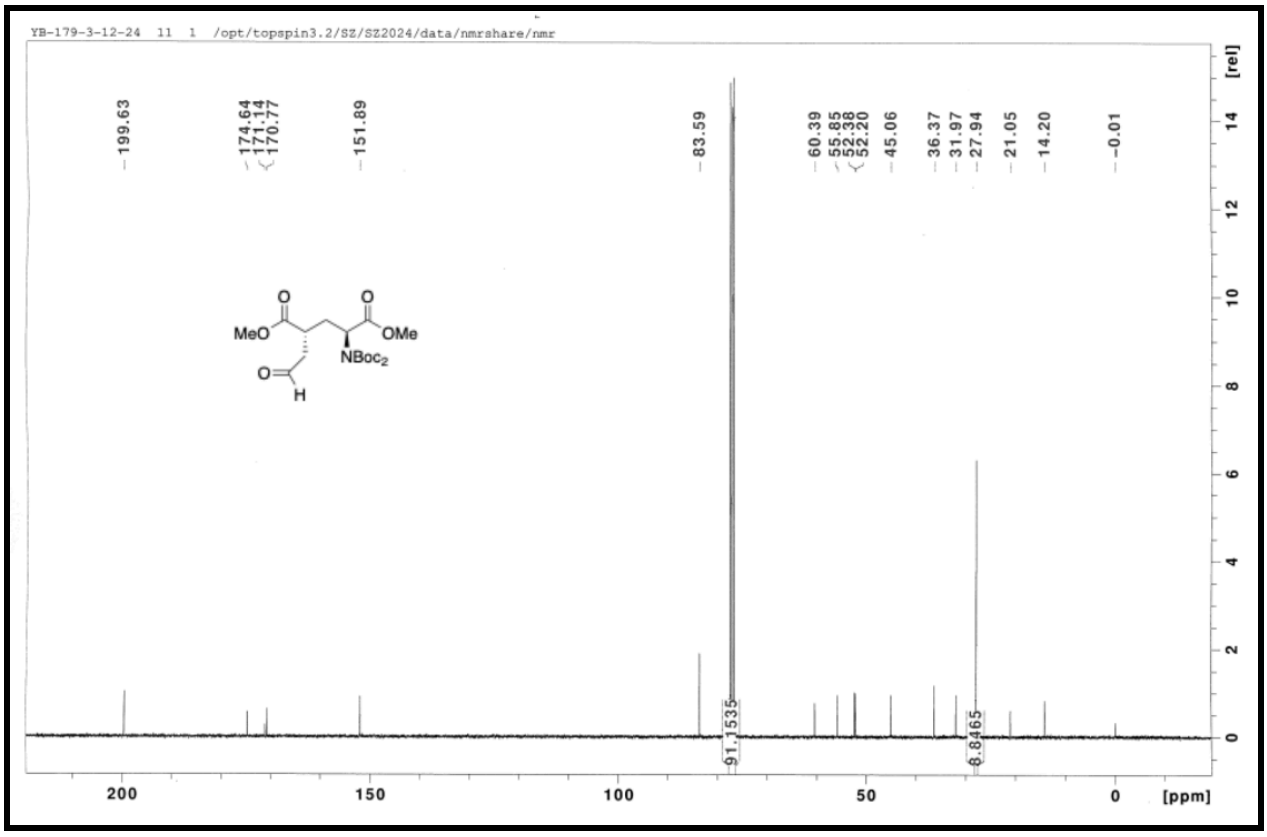

2-(((tert-Butyldimethylsilyl)oxy)methyl)phenol (<u>14</u>)

To a solution of commercially available 2-hydroxybenzyl alcohol (2 g, 0.016 mol) dissolved in DMF (10 mL) was added a solution of TBSCl (2.6 g, 0.016 mol) in DMF (2 mL) and a solution of imidazole (3.3 g, 0.048 mol) in DMF (2 mL). The reaction was stirred for 1 hour. The mixture was extracted with EA three times (15 mL) and the organic layer was dried over Na_2SO_4, concentrated under vacuum, and purified through flash chromatography (Hexane/EA 10:1 to 5:1) to give **14** as a viscous yellow liquid (2.04 g, 52% yield).

^{1}H NMR: δ 7.92 (s, 1H), 7.04 (dd, *J* = 8 Hz, 1H), 6.81 (d, *J* = 8 Hz, 1H), 6.73 (d, *J* = 8 Hz, 1H), 6.68 (dd, *J* = 8 Hz, 1H), 4.77 (s, 2H), 0.79 (s, 9H), 0.00 (s, 6H).

^{13}C NMR δ 156.64, 128.94, 126.66, 124.10, 119.59, 116.65, 65.92, 25.73, 18.14, -5.33.

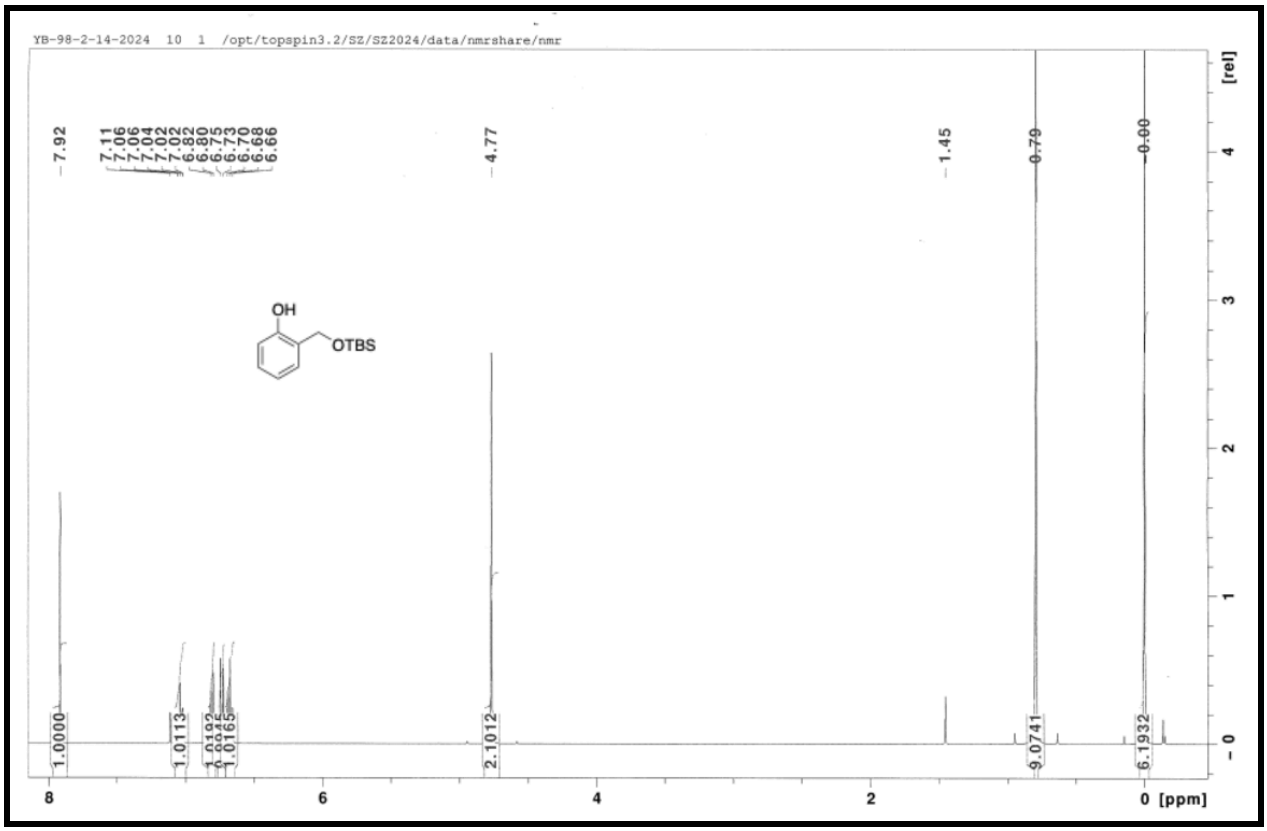
YB-98-2-14-2024 10 1 /opt/topspin3.2/SZ/SZ2024/data/nmrshare/nmr
7.92
7.11
7.06
7.06
7.04
7.02
7.02
6.82
6.80
6.75
6.73
6.70
6.68
6.66
4.77
1.45
0.79
0.00
OH
OTBS
1.0000
1.0113
1.0102
1.0045
1.0165
2.1012
9.0741
6.1932
[rel]
[ppm]

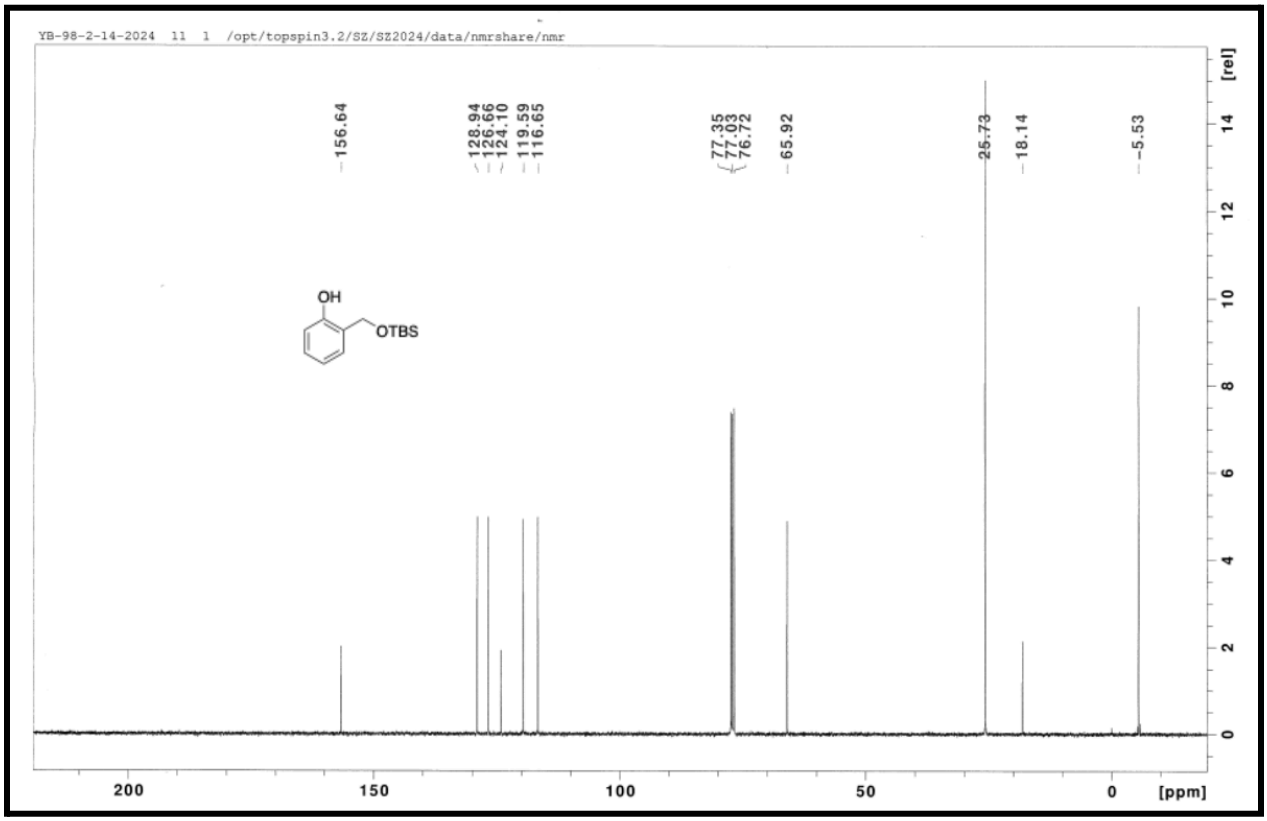
YB-98-2-14-2024 11 1 /opt/topspin3.2/SZ/SZ2024/data/nmrshare/nmr
156.64
128.94
126.66
124.10
119.59
116.65
77.35
77.03
76.72
65.92
25.73
18.14
-5.53
OH
OTBS
[rel]
[ppm]

Compound 15

To a solution of **14** (1.06 g, 0.004 mol) dissolved in DMF (20 mL) was added NaH (193.1 mg, 60% dispersion in mineral oil, 0.005 mmol) dissolved in DMF (2 mL) at 0 ºC. The reaction mixture was stirred for 15 minutes before the addition of a solution of R-Br (0.006 mol) in DMF (2 mL) and added at 0 ºC. The mixture was stirred for 1 hour at 0 ºC, quenched with H_2O, and extracted three times with hexane (10 mL). The organic layer was dried over Na_2SO_4, concentrated under vacuum, and purified by flash chromatography (Hexane/EA 10:1 to 5:1) to give **15** as a clear liquid (2.0 g, 95% yield).

NMR characterization data was not included due to proprietary substitutions.

Compound 16

To a solution of **15** (0.977 g, 0.021 mol) in THF (100 mL) was added TBAF (3.1 mmol, 3.1 mL) at room temperature. The reaction was stirred for 1 hour at room temperature and then quenched with water. The mixture was extracted with EA, dried over Na_2SO_4, concentrated under vacuum, and purified by flash chromatography (Hexane/EA 20:1 to 5:1) to give **16** as a transparent liquid (376.3 mg, 51% yield).

NMR characterization data was not included due to proprietary substitutions.

Compound 18

To a solution of L-leucine hydrochloride salt (500 mg, 2.7 mmol) in DCM (15 mL) was added sodium carbonate (10 mL) and triphosgene (260 mg, 0.9 mmol) at 0 ºC. The reaction was stirred for 1 hour at room temperature, then extracted twice with 15 mL of DCM, dried over Na_2SO_4, and concentrated under vacuum. To a solution of **17** in THF (5 mL) was added a

solution of Intermediate A (260 mg, 0.7 mmol) in THF (3 mL) and triethylamine (0.3 mL, 2.1 mmol). The reaction mixture was stirred at 70 ºC for three hours. The reaction mixture was concentrated under vacuum and purified by flash chromatography (Hexane/EA 4:1 to 2:1), to give **18** (367 mg, 0.78 mmol, 98% yield).

NMR characterization data was not included due to proprietary substitutions.

Abbreviations

Boc = *tert*-butyloxycarbonyl

DCM = Dichloromethane

DMF = Dimethylformamide

EA = Ethyl acetate

m-CPBA = *meta*-Chloroperoxybenzoic acid

Glu = Glutamic Acid

LC/MS = Liquid Chromatography/ Mass Spectroscopy

MeCN = Acetonitrile

MERS = Middle Eastern Respiratory Syndrome

N-Boc-Glu-OMe = N-Boc-L-Glutamic Acid dimethyl ester

NMO = *N*-Methylmorpholine *N*-oxide

NMR = Nuclear magnetic resonance

PI = Protease Inhibitor

Rt = Room Temperature

SARS = Severe acute respiratory syndrome

TBAF = Tetra-*n*-butylammonium fluoride

TBS = *tert*-Butylsilyl

TBSCl = *tert*-Butylsilyl chloride

THF = Tetrahydrofuran

TLC = Thin-layer chromatography

TMS = Trimethylsilyl

References

1) United States COVID-19 Hospitalizations, Deaths, Emergency Department (ED) Visits, and Test Positivity by Geographic Area. Covid Data Tracker. *Centers for Disease Control and Prevention.* https://covid.cdc.gov/covid-data-tracker/#maps_percent-covid-deaths (accessed March 19, 2024).
2) Coronavirus World Map: Tracking the Global Outbreak. *New York Times.* https://www.nytimes.com/interactive/2021/world/covid-cases.html (accessed March 13, 2024).
3) Alimohamadi, Y; Taghdir, M; Sepandi, M. The estimate of the basic reproduction number for novel coronavirus disease (COVID-19): a systematic review and meta-analysis. *J. Prev. Med. Public Health*. **2020**, *53*(3), 151-157.
4) Alimohamadi, Y; Taghdir, M; Sepandi, M; Hodsamirudsari, H. Determine the most common clinical symptoms in COVID-19 patients: a systematic review and meta-analysis. *J. Prev. Med. Hyg*. **2020**. *61*(3), 304–E312.
5) Finkel, Y; Mizrahi, O; Nachson, A; Weingarten-Gabbay, S; Morgenstern, D; Yahalom-Ronen, Y; Tamir, H; Achdout, H; Stein, D; Israeli, O; Beth-Din, A; Melamed, S; Weiss, S; Israely, T; Paran, N; Schwartz, M; Stern-Ginossar, N. The coding capacity of

SARS-CoV-2. *Nature*. **2021**. *589*. 125-130.

6) Li, X.; Song, Y. Structure and function of SARS-CoV and SARS-CoV-2 main proteases and their inhibition: A comprehensive review. *Eur. J. Med. Chem*. **2023**, *260*, 115772.
7) Chen, S; Duan, X; Lacko, L. Druggable targets and therapeutic development for COVID-19. *Front. Chem*. **2022**. *10*. 963701.
8) Mukherjee, R. Proteases of SARS Coronaviruses. *Enc. Cell Bio.* **2023**, *2*(1), 930-941.
9) Zhang, L; Din, L; Sun, X; Curth, U; Drosten, C; Sauerhering, L; Becker, S; Rox, K; Hilgenfeld, R. Crystal structure of SARS-CoV-2 main protease provides a basis for design of improved α-ketoamide inhibitors. *Science.* **2020**, *368*(6489), 409-412.
10) Wei, G; Gao, K; Wang, R; Chen, J; Tepe, J; Huang, F. Perspectives on SARS-CoV-2 Main Protease Inhibitors. *J. Med. Chem.* **2021**, *64*(21), 16922-16955.
11) Xing, D; Chen, W; Liang, B; Wu, X; Li, L; Wang, C. Advances and challenges in using nirmatrelvir and its derivatives against SARS-CoV-2 infection. *J. Pharm. Anal*. **2023**, *13*(3), 255-261.
12) Amblard, F; LeCher, J; De, R; Zhou, S; Liu, P; Goh, S; Tao, S; Patel, D; Downs-Bowen, J; Zandi, K; Zhang, H; Chaudry, G; McBrayer, T; Muczynski, M; Al-Homoudi, A; Engel, J; Lan, S; Sarafianos, S; Kovari, L; Schinazi, R. Synthesis and biological evaluation of novel peptidomimetic inhibitors of the coronavirus 3C-like protease. *Eur. J. Med. Chem*. **2024**. *268*, 116263.
13) Fu, L; Ye, F; Feng, Y; Yu, F; Wang, Q; Wu, Y; Zhao, C; Sun, H; Huang, B; Niu, P; Song, H; Shi, Y; Li, X. Both Boceprevir and GC376 efficaciously inhibit SARS-CoV-2 by targeting its main protease. *Nat. Comm.* **2020**, *11*(4417).
14) Olsen, S; Huang, T; Drag, M; Lijia, J; Cano, K; Lv, Z. Targeting SARS-CoV-2 Proteases

for COVID-19 Antiviral Development. *Front*. *Chem*. **2021**. *9*. 81965.

15) Jiang, X; Su, H; Shang, W; Zhou, F; Zhang, Y; Zhao, W; Zhang, Q; Xie, H; Jiang, L; Nie, T; Yang, F; Xiong, M; Huang, X; Li, M; Chen, P; Peng, S; Xiao, G; Jiang, H; Tang, R; Zhang, L; Shen, J; Xu, Y. Structure-based development and preclinical evaluation of the SARS-CoV-2 3C-like protease inhibitor simnotrelvir. *Nat. Commun.* **2023.** *14*, 6463.

16) Halford, B. How Pfizer scientists transformed an old drug lead into a COVID-19 antiviral. *Chemical & Engineering News.* https://cen.acs.org/pharmaceuticals/drug-discovery/How-Pfizer-scientists-transformed-an-old-drug-lead-into-a-COVID-19-antiviral/100/i3 (accessed March 13, 2024).

17) Vuong, W; Vederas, J. Improved synthesis of a cyclic glutamine analogue used in antiviral agents targeting 3C and 3CL proteases including SARS-CoV-2 M^{Pro}. *J. Org. Chem.* 2021, *86*(18), 13104-13110.

18) Jacobsen, E; Hansen, K. Leighton, J. On the mechanism of asymmetric nucleophilic ring-opening of epoxides catalyzed by (Salen)Cr^{III} complexes. *J. Am. Chem. Soc.* **1996**, *118*(44), 10924-10925.

19) Jacobsen, E; Leighton, J. Efficient synthesis of (R)-4-((Trimethylsilyl)oxy)-2-cyclopentenone by enantioselective catalytic epoxide Ring opening. *J. Org. Chem*. **1996**. *61*(1). 389-390.

20) Shabat, D; Baran, P; Perry-Feigenbaum, R.The pyridinone-methide elimination. *Org. & Biom. Chem*. **2009**. *7*. 4825-4828.